ARR No. L5F06

NATIONAL ADVISORY COMMITTEE FOR AERONAUTICS

WARTIME REPORT

ORIGINALLY ISSUED
June 1945 as
Advance Restricted Report L5F06

WIND-TUNNEL INVESTIGATION OF CONTROL-SURFACE CHARACTERISTICS

XXII - MEDIUM AND LARGE AERODYNAMIC BALANCES OF TWO NOSE SHAPES AND A PLAIN OVERHANG USED WITH A 0.20-AIRFOIL-CHORD FLAP ON AN NACA 0009 AIRFOIL

By John M. Riebe and Elizabeth G. McKinney

Langley Memorial Aeronautical Laboratory
Langley Field, Va.

WASHINGTON

NATIONAL ADVISORY COMMITTEE FOR AERONAUTICS

ADVANCE RESTRICTED REPORT

WIND-TUNNEL INVESTIGATION OF CONTROL-SURFACE CHARACTERISTICS

XXII - MEDIUM AND LARGE AERODYNAMIC BALANCES OF TWO NOSE SHAPES AND A PLAIN OVERHANG USED WITH A 0.20-AIRFOIL-CHORD FLAP ON AN NACA 0009 AIRFOIL

By John M. Riebe and Elizabeth G. McKinney

SUMMARY

Blunt-nose and elliptical-nose overhangs of 0.35 and 0.50 flap chord and a plain overhang on a flap having a chord of 0.20 airfoil chord have been tested in two-dimensional flow on an NACA 0009 airfoil. The results of the tests are presented as aerodynamic section characteristics for several flap deflections with the gap at the flap nose sealed or unsealed. Tests were made also to determine the effectiveness of a tab of 0.20 flap chord on the plain sealed flap and on a sealed flap having an elliptical overhang of 0.35 flap chord. The pressure difference across the flap seal was also determined for the plain sealed flap.

The results indicated that the plain sealed flap had the largest lift-curve slope, whereas the slopes for the 0.50-flap-chord overhangs were the same as or slightly larger than for the 0.35-flap-chord overhangs. A reduction in slope caused by unsealing the flap gap increased with balance chord.

The change in lift coefficient with flap deflection generally increased when the gap was sealed and when the balance nose shape was changed from elliptical to blunt.

Sealing the flap gap generally made the variation of flap hinge-moment coefficient with angle of attack and with flap deflection more negative. Changing the nose shape from blunt to elliptical made the variation of the flap hinge-moment coefficient with angle of attack more negative for the sealed gap and more positive

for the unsealed gap. At small flap deflections, the variation of flap hinge-moment coefficient with flap deflection was more negative for the elliptical-nose than for the blunt-nose flap; at large deflections, however, this variation was more negative for the blunt-nose flap.

The change of flap hinge-moment coefficient with flap deflection for the unsealed blunt-nose overhang had a larger variation with balance chord than the change of flap hinge-moment coefficient with angle of attack; for the sealed blunt-nose overhang, these variations were about the same in the range of balance chord from 0.35 to 0.50 flap chord. For the sealed and unsealed elliptical-nose overhangs, the change of flap hinge-moment coefficient with angle of attack had a larger variation than the change of flap hinge-moment coefficient with flap deflection.

INTRODUCTION

The NACA is conducting an extensive investigation to determine the characteristics of various types of flap arrangement suitable for use as control surfaces and to provide data for design purposes. The investigation, which was made in the Langley 4- by 6-foot vertical tunnel, has included tests of modifications of flap profile, trailing-edge angle, gap size, flap nose shape, and balance chord; however, most of these tests have been made in two-dimensional flow with a flap having a chord 30 percent of the airfoil chord (0.30c). The present tests have extended the investigation of balance chord and flap nose shape, which was reported in reference 1 for a 0.40c flap, to a 0.20c flap. Data on the pressure across the flap nose seal and a method of applying these pressure data in the design of internal balances are presented. Tab data are presented for the plain flap and for a flap with aerodynamic balance.

SYMBOLS

The coefficients and symbols used in this paper are defined as follows:

c_l airfoil section lift coefficient (l/qc)

c_{d_o} airfoil section profile-drag coefficient (d_o/qc)

c_m airfoil section pitching-moment coefficient (m/qc^2)

c_{h_f} flap section hinge-moment coefficient (h_f/qc_f^2)

c_{h_t} tab section hinge-moment coefficient (h_t/qc_t^2)

P_R resultant pressure coefficient $\left(\frac{p_L - p_U}{q}\right)$

where

l airfoil section lift

d_o airfoil section profile drag

m airfoil section pitching moment about quarter-chord point of airfoil; positive moment moves nose of airfoil up

h_f flap section hinge moment about flap hinge axis; positive moment moves trailing edge down

h_t tab section hinge moment about tab hinge axis; positive moment moves trailing edge down

c chord of basic airfoil with flap and tab neutral

c_f flap chord from flap hinge axis to trailing edge

c_t tab chord from tab hinge axis to trailing edge

q free-stream dynamic pressure

p_L static pressure on lower surface of seal

p_U static pressure on upper surface of seal

and

c_b balance chord

α_o angle of attack for airfoil of infinite aspect ratio; positive when nose of airfoil moves up

δ_f flap deflection with respect to airfoil; positive when trailing edge is deflected down

δ_t tab deflection with respect to flap; positive when trailing edge is deflected down

$$\alpha_{\delta_f} = \left(\frac{\partial \alpha_o}{\partial \delta_f}\right)_{c_l, \delta_t}$$

$$c_{l_\alpha} = \left(\frac{\partial c_l}{\partial \alpha_o}\right)_{\delta_f, \delta_t}$$

$$c_{l_{\delta_f}} = \left(\frac{\partial c_l}{\partial \delta_f}\right)_{\alpha_o, \delta_t}$$

$$c_{l_{\delta_t}} = \left(\frac{\partial c_l}{\partial \delta_t}\right)_{\alpha_o, \delta_f}$$

$$c_{h_{f_\alpha}} = \left(\frac{\partial c_{h_f}}{\partial \alpha_o}\right)_{\delta_f, \delta_t}$$

$$c_{h_{f_{\delta_f}}} = \left(\frac{\partial c_{h_f}}{\partial \delta_f}\right)_{\alpha_o, \delta_t}$$

$$c_{h_{f_{\delta_t}}} = \left(\frac{\partial c_{h_f}}{\partial \delta_t}\right)_{\alpha_o, \delta_f}$$

$$\left(c_{m_{c_l}}\right)_{\delta_f, \delta_t} = \left(\frac{\partial c_m}{\partial c_l}\right)_{\delta_f, \delta_t}$$

$$\left(c_{m_{c_l}}\right)_{\alpha, \delta_t} = \left(\frac{\partial c_m}{\partial c_l}\right)_{\alpha_o, \delta_t}$$

The subscripts outside the parentheses represent the factors held constant during the measurement of the parameters.

APPARATUS AND MODEL

The tests were made in the Langley 4- by 6-foot vertical tunnel described in reference 2 and modified as described in reference 3.

The model, when mounted in the tunnel, completely spanned the test section except for $\frac{1}{32}$-inch clearance gaps between the model and the tunnel walls. With this type of installation, two-dimensional flow is closely approximated and the section characteristics of the airfoil, flap, and tab may be determined. The model was attached to the balance frame by torque tubes that extended through the sides of the tunnel. The angle of attack was set from outside the tunnel by rotating the torque tubes with an electric drive. Flap deflections were set by an electrical position indicator, and tab deflections were set by a templet. The hinge moments of the flap were measured with a special torque-rod balance built into the model.

Tab hinge moments were measured by an electrical strain gage installed in the model. For tests of the plain sealed flap, the pressure difference across the gap seal was measured on a manometer.

The model (fig. 1), which had a chord of 2 feet and a span of 4 feet, was made of laminated mahogany (except for a steel tab), was aerodynamically smooth, and conformed to the NACA 0009 profile (table I). It was equipped with a 0.20c flap and a $0.20c_f$ plain tab. The flap had a plain nose with a radius that was approximately one-half the airfoil thickness at the flap hinge axis or was fitted with $0.35c_f$ or $0.50c_f$ blunt-nose or elliptical-nose aerodynamic balances. The elliptical nose, the ordinates of which are given in table II, was a true ellipse tangent to the airfoil contour at the flap hinge axis. The radii shown in figure 1 determined the blunt and plain noses.

The various nose blocks were interchangeable and were fastened to the flap at the hinge axis. In order to keep the gap at the flap nose at 0.005c, blocks corresponding to each balance chord were attached to the airfoil just ahead of the balance. For the sealed-gap tests, airtight fabric was fastened between the flap nose and the airfoil.

The $0.20c_f$ tab had a nose radius approximately one-half the airfoil thickness at the tab hinge axis. The tab gap was 0.001c for all the tests.

TESTS

A dynamic pressure of 15 pounds per square foot, which corresponds to a velocity of about 76 miles per hour at standard sea-level conditions, was used throughout the tests. The test Reynolds number was 1,430,000 and the effective Reynolds number was approximately 2,760,000. (Effective Reynolds number = Test Reynolds number × Turbulence factor. The turbulence factor for the Langley 4- by 6-foot vertical tunnel is 1.93.) The Mach number for the tests was about 0.10.

The maximum error in angle of attack appears to be $\pm 0.2^\circ$. It is estimated that the flap and tab deflections were set within $\pm 0.2^\circ$.

An experimentally determined tunnel correction was applied to the lift coefficient. In accordance with a theoretically derived analysis similar to that presented in reference 4 for finite-span models, the angle of attack and the hinge-moment coefficient were corrected for the effect of streamline curvature induced by the tunnel walls. The increments of drag coefficient are believed to be reasonably independent of tunnel effect, although the absolute value is subject to an unknown correction. Inaccuracies in model construction and assembly of interchangeable blocks probably caused the small flap hinge moment at $\alpha_o = 0^\circ$ and $\delta_f = 0^\circ$.

A summary of information for convenience in locating the data for the various model configurations is presented in table III.

RESULTS AND DISCUSSION

Lift

The lift-coefficient curves for the plain flap and for the flaps with various overhangs are given in figures 2 to 11 for the flap gaps both sealed and unsealed. These curves were nonlinear at large flap deflections. The flaps with elliptical-nose overhangs generally developed lift to larger flap deflections than those with blunt-nose overhangs.

Parameter values obtained from figures 2 to 11 are summarized in table IV. The variations with balance chord of the lift parameters c_{l_α}, $c_{l_{\delta_f}}$, and α_{δ_f} are given in figure 12.

With the gaps sealed and unsealed, the plain flap had the largest values of the slope of the lift curve c_{l_α}, whereas the values of c_{l_α} for the $0.50c_f$ overhangs were the same as or larger than for the $0.35c_f$ overhangs. This variation was similar for the 0.40c flap (reference 1). A reduction in c_{l_α} caused by unsealing the gap increased with balance chord.

The value of $c_{l_{\delta_f}}$ was usually larger for the blunt than for the elliptical nose. Except for the flap with the $0.50c_f$ blunt-nose overhang, sealing the gap increased $c_{l_{\delta_f}}$.

The flap lift effectiveness parameter α_{δ_f} decreased as the balance chord increased, except for the flap with the unsealed blunt-nose overhang, and was usually larger for the blunt-nose than for the elliptical-nose overhang. Sealing the gap increased α_{δ_f} for the elliptical-nose overhang and the plain flap but generally decreased it for the blunt-nose overhang. The values of α_{δ_f} given in table IV and figure 12 were measured over a small flap deflection range at $c_l = 0$ and therefore are mainly useful as a comparison of the various configurations tested.

Hinge Moment

The curves of flap hinge-moment coefficient as a function of angle of attack at constant flap deflections are presented in figures 2 to 11 for the plain flap and for the flaps with various overhangs. No appreciable flap oscillations were noticed throughout the flap deflection range tested, although such oscillations occurred on the 0.40c flap (reference 1).

The hinge-moment parameters $c_{h_{f_\alpha}}$ and $c_{h_{f_{\delta_f}}}$ presented in table IV and plotted against balance chord in figure 13 indicate that the $0.50c_f$ blunt-nose overhang was overbalanced $\left(c_{h_{f_{\delta_f}}}\text{ was positive}\right)$ and had a positive $c_{h_{f_\alpha}}$ for the gap sealed and unsealed. (Values of $c_{h_{f_\alpha}}$ were determined at $\alpha_o = 0^o$ and at $\delta_f = 0^o$ and values of $c_{h_{f_{\delta_f}}}$ were determined at $\alpha_o = 0^o$ and small flap deflections.) The 0.20c flap was found to be overbalanced for conditions similar to those for which the 0.40c flap tested on the same airfoil (reference 1) had been overbalanced. For the flap with the $0.50c_f$ overhang, $c_{h_{f_{\delta_f}}}$ could be made negative by the use of a tab deflected in the same direction as the flap.

The $0.50c_f$ elliptical-nose overhang, with sealed and unsealed gap, had a positive $c_{h_{f_\alpha}}$ at $\delta_f = 0^o$; at larger flap deflections, however, an increase in angle of attack or flap deflection generally gave a negative increment of hinge-moment coefficient (figs. 10 and 11). For the $0.50c_f$ blunt-nose overhang, flap deflections up to approximately 15^o gave positive increments of hinge-moment coefficient; changing the flap to larger deflections gave negative increments.

Figure 13 indicates that, for the unsealed blunt-nose overhang, $c_{h_{f_{\delta_f}}}$ had a larger variation with balance chord than $c_{h_{f_\alpha}}$; for the sealed blunt-nose overhang, the variations of $c_{h_{f_\alpha}}$ and $c_{h_{f_{\delta_f}}}$ were about the same in the range of balance chord from $0.35c_f$ to $0.50c_f$. For the sealed and unsealed elliptical-nose overhangs, $c_{h_{f_\alpha}}$ had a larger variation than $c_{h_{f_{\delta_f}}}$.

Changing the nose shape from blunt to elliptical made $c_{h_{f_\alpha}}$ more negative for the sealed gap and more positive for the unsealed gap. Changing the nose shape from blunt to elliptical also made $c_{h_{f_{\delta_f}}}$ more negative at small flap deflections and less negative at large flap deflections.

Sealing the gap at the flap nose generally made $c_{h_{f_{\delta_f}}}$ and $c_{h_{f_\alpha}}$ more negative.

Since the aspect-ratio corrections for streamline curvature are always positive (reference 5) and since the hinge-moment parameters are very small and the signs are critical for several of the flaps with overhangs, the slopes may change from negative to positive and produce an overbalanced flap on a finite-span wing.

Because the hinge-moment parameters shown in table IV represent the slopes of the curves at $\delta_f = 0^{\circ}$ and $\alpha_o = 0^{\circ}$, these parameters should be used mainly as an indication of the relative merits of the different flap nose shapes. Because the tabulated slopes are valid for only a small range, the curves of hinge-moment coefficient should be used, rather than the tabulated parameters, in the calculation of the characteristics of a control surface.

Pitching Moment

Values of the pitching-moment parameters $\left(c_{m_{c_l}}\right)_{\delta_f,\delta_t}$ and $\left(c_{m_{c_l}}\right)_{\alpha,\delta_t}$ are shown in table IV and indicate the position of the aerodynamic center with respect to the 0.25c point. When the lift was varied by changing the angle of attack at $\delta_f = 0^{\circ}$, the aerodynamic center for the plain sealed flap was located at the 0.25c point; the aerodynamic center for the balanced flap with sealed gap, regardless of balance chord or nose shape, was near the 0.24c point. The effect of unsealing the gap was to move the aerodynamic center 0.01c forward.

The center-of-lift positionsdue to flap deflections up to approximately 15° are given in the following table:

Gap	Center-of-lift position caused by flap deflection (percent c)				
	Plain overhang	$0.35c_f$ overhang		$0.50c_f$ overhang	
		Blunt nose	Elliptical nose	Blunt nose	Elliptical nose
Sealed	46	45	44	44	46
0.005c	46	44	47	43	50

This table indicates that the center-of-lift position was the same for the plain flap whether the gap was sealed or unsealed. The effect of unsealing the gap or of increasing the balance chord was to move the center-of-lift position due to flap deflection forward on the blunt-nose and rearward on the elliptical-nose flap. The center-of-lift position caused by flap deflection is a function of the aspect ratio (references 5 and 6) and moves rearward as the aspect ratio decreases.

Drag

Because of an undetermined tunnel correction, the measured values of drag cannot be considered absolute, but relative values of drag are thought to be independent of tunnel effect.

The increments of section profile-drag coefficient caused by flap deflection are presented in figure 14 for the plain flap and in figure 15 for the $0.35c_f$ and $0.50c_f$ blunt-nose overhangs.

Tab Characteristics

Because the characteristics for a tab on a flap with aerodynamic balance, in general, are similar to those for a tab on a plain flap (references 3 and 7) and are usually independent of flap nose shape (reference 7), only a limited investigation of tab characteristics has been made.

The aerodynamic section characteristics as a function of angle of attack, for a tab ratio $\frac{\partial \delta_t}{\partial \delta_f} = \pm 1$, are presented in figures 16 and 17 for the plain sealed flap and for the $0.35c_f$ sealed elliptical-nose overhang, respectively. The values of $c_{h_{f_{\delta_t}}}$ for the $0.35c_f$ elliptical-nose overhang (figs. 7 and 17) were, in general, the same as or slightly less than the values for the plain flap (figs. 3 and 16). With the tab deflected and with $\delta_f = 0^\circ$ (fig. 18), $c_{l_{\delta_t}}$ was 0.017 and $c_{h_{f_{\delta_t}}}$ was -0.012 for the plain sealed flap. The tab, in general, was slightly more effective in producing lift on the plain flap than on the flap with the $0.35c_f$ overhang. The effectiveness of the tab in changing the flap hinge moment decreased with tab deflection. A comparison of figures 3 and 16 with figure 18 showed that the tab effectiveness generally was the same whether the flap was at 0° or deflected.

Pressure Difference across Plain-Flap Seal

The variation of resultant pressure coefficient across the plain-flap nose seal with angle of attack at constant flap deflections is shown in figure 19. The change in resultant pressure coefficient with angle of attack $\left(\frac{\partial P_R}{\partial \alpha_o}\right)_{\delta_f, \delta_t}$ was found to increase with flap deflection.

The data of figure 19 can be used with those of figure 3 to determine the flap section hinge-moment coefficient at a given angle of attack and flap deflection for a 0.20c flap with an internal balance on an NACA 0009 airfoil. It can be shown that

$$\left(c_{h_f}\right)_{IB} = c_{h_f} + P_R K \qquad (1)$$

where

$\left(c_{h_f}\right)_{IB}$ section hinge-moment coefficient for flap with internal balance

c_{h_f} section hinge-moment coefficient for plain flap with gap sealed, obtained from figure 3

P_R resultant pressure coefficient, obtained from figure 19

K constant, obtained from figure 20 $\left(\dfrac{\left(\dfrac{c_b'}{c_f}\right)^2 - \left(\dfrac{t}{c_f}\right)^2}{2}\right)$

t semithickness at hinge axis

c_b' balance chord plus one-half gap width

The hinge-moment parameters $c_{h_{f_\alpha}}$ and $c_{h_{f_{\delta_f}}}$ determined from flap hinge-moment coefficients obtained by equation (1) are plotted in figure 13 for internal balances of various chords.

CONCLUSIONS

Blunt-nose and elliptical-nose overhangs of 35 and 50 percent flap chord $\left(0.35c_f \text{ and } 0.50c_f\right)$ and a plain overhang on a flap having a chord 20 percent of the airfoil chord (0.20c) have been tested in two-dimensional flow on an NACA 0009 airfoil. A limited investigation was also made of the characteristics of a $0.20c_f$ plain tab. The results of the tests indicated the following conclusions:

1. The slope of the lift curve was largest for the plain sealed flap, whereas the slopes for the $0.50c_f$ overhangs were the same as or slightly larger than for the $0.35c_f$ overhangs. A reduction in slope caused by unsealing the gap increased with balance chord.

2. The variation of lift coefficient with flap deflection generally increased when the gap was sealed and when the nose was changed from elliptical to blunt.

3. The flap lift effectiveness parameter α_{δ_f} generally decreased when the overhang chord was increased and was usually larger for the blunt-nose than for the elliptical-nose overhang. Sealing the gap increased α_{δ_f}

for the plain flap and for the elliptical-nose overhang but generally decreased it for the blunt-nose overhang.

4. Sealing the gap at the flap nose made the variation of flap hinge-moment coefficient with angle of attack more negative; changing the nose shape from blunt to elliptical made this variation more negative for the sealed gap and more positive for the unsealed gap.

5. The variation of flap hinge-moment coefficient with flap deflection was generally more negative with a sealed gap than with an unsealed gap. Changing the nose shape from blunt to elliptical made this variation more negative at small flap deflections and less negative at large flap deflections.

6. The change of flap hinge-moment coefficient with flap deflection, for the unsealed blunt-nose overhang, had a larger variation with balance chord than the change of flap hinge-moment coefficient with angle of attack; for the sealed blunt-nose overhang, these variations were about the same in the range of balance chord from $0.35c_f$ to $0.50c_f$. For the sealed and unsealed elliptical-nose overhangs, the change of flap hinge-moment coefficient with angle of attack had a larger variation than the change of flap hinge-moment coefficient with flap deflection.

7. For all conditions, unsealing the gap moved the aerodynamic center forward about 1 percent airfoil chord. Unsealing the gap or increasing the balance chord moved the center-of-lift position due to flap deflection forward for the blunt-nose and rearward for the elliptical-nose flap.

8. The tab was slightly more effective in changing the lift and the flap hinge moment on the plain flap than on the flap with $0.35c_f$ elliptical-nose overhang.

Langley Memorial Aeronautical Laboratory
National Advisory Committee for Aeronautics
Langley Field, Va.

REFERENCES

1. Riebe, John M., and Church, Oleta: Wind-Tunnel Investigation of Control-Surface Characteristics. XXI - Medium and Large Aerodynamic Balances of Two Nose Shapes and a Plain Overhang Used with a 0.40-Airfoil-Chord Flap on an NACA 0009 Airfoil. NACA ARR No. L5C01, 1945.

2. Wenzinger, Carl J., and Harris, Thomas A.: The Vertical Wind Tunnel of the National Advisory Committee for Aeronautics. NACA Rep. No. 387, 1931.

3. Sears, Richard I., and Gillis, Clarence L.: Wind-Tunnel Investigation of Control-Surface Characteristics. VIII - A Large Aerodynamic Balance of Two Nose Shapes Used with a 30-Percent-Chord Flap on an NACA 0015 Airfoil. NACA ARR, July 1942.

4. Swanson, Robert S., and Toll, Thomas A.: Jet-Boundary Corrections for Reflection-Plane Models in Rectangular Wind Tunnels. NACA ARR No. 3E22, 1943.

5. Swanson, Robert S., and Gillis, Clarence L.: Limitations of Lifting-Line Theory for Estimation of Aileron Hinge-Moment Characteristics. NACA CB No. 3L02, 1943.

6. Ames, Milton B., Jr., and Sears, Richard I.: Determination of Control-Surface Characteristics from NACA Plain-Flap and Tab Data. NACA Rep. No. 721, 1941.

7. Ames, Milton B., Jr.: Wind-Tunnel Investigation of Control-Surface Characteristics. III - A Small Aerodynamic Balance of Various Nose Shapes Used with a 30-Percent-Chord Flap on an NACA 0009 Airfoil. NACA ARR, Aug. 1941.

TABLE I

ORDINATES FOR NACA 0009 AIRFOIL

[Stations and ordinates in percent airfoil chord]

Station	Upper surface	Lower surface
0	0	0
1.25	1.42	-1.42
2.5	1.96	-1.96
5	2.67	-2.67
7.5	3.15	-3.15
10	3.51	-3.51
15	4.01	-4.01
20	4.30	-4.30
25	4.46	-4.46
30	4.50	-4.50
40	4.35	-4.35
50	3.97	-3.97
60	3.42	-3.42
70	2.75	-2.75
80	1.97	-1.97
90	1.09	-1.09
95	.60	-.60
100	(.10)	(-.10)
100	0	0
L.E. radius: 0.89		

NATIONAL ADVISORY
COMMITTEE FOR AERONAUTICS

TABLE II

ORDINATES FOR 0.35c_f AND 0.50c_f ELLIPTICAL-NOSE OVERHANGS

[Stations measured from forward end of overhang; stations and ordinates measured in percent airfoil chord]

0.35c_f overhang		0.50c_f overhang	
Station	Ordinate	Station	Ordinate
0	0	0	0
.03	.21	.03	.21
.12	.42	.15	.42
.18	.62	.36	.62
.50	.83	.65	.83
.81	1.04	1.05	1.04
1.22	1.25	1.58	1.25
1.75	1.46	2.25	1.46
2.48	1.67	3.17	1.67
2.85	1.75	3.63	1.75
3.30	1.83	4.18	1.83
3.90	1.92	4.87	1.92
4.92	2.00	5.86	2.00
5.67	2.02	6.70	2.04
6.42	2.00	7.67	2.06
7.00	1.97	8.64	2.04
		9.48	2.00
		10.00	1.97

NATIONAL ADVISORY
COMMITTEE FOR AERONAUTICS

TABLE III

MODEL CONFIGURATIONS TESTED

[NACA 0009 airfoil with 0.20c flap and 0.20c_f plain tab; tab gap, 0.001c]

Overhang	Flap gap	δ_f range (deg)	δ_t range (deg)	Figure
Plain	0.005c	0 to 30	0	2, 14
Plain	Sealed	0 to 30	0	3, 14, 19
0.35c_f blunt nose	0.005c	0 to 25	0	4, 15
0.35c_f blunt nose	Sealed	0 to 25	0	5, 15
0.35c_f elliptical nose	0.005c	0 to 25	0	6
0.35c_f elliptical nose	Sealed	0 to 25	0	7
0.50c_f blunt nose	0.005c	0 to 25	0	8, 15
0.50c_f blunt nose	Sealed	0 to 20	0	9, 15
0.50c_f elliptical nose	0.005c	0 to 25	0	10
0.50c_f elliptical nose	Sealed	0 to 20	0	11
Plain	Sealed	0 to 30	-30 to 30	16
0.35c_f elliptical nose	Sealed	0 to 20	-20 to 20	17
Plain	Sealed	0	0 to 30	18

NATIONAL ADVISORY
COMMITTEE FOR AERONAUTICS

TABLE IV

PARAMETER VALUES FOR 0.20c FLAP WITH PLAIN, $0.35c_f$, AND $0.50c_f$ OVERHANGS ON NACA 0009 AIRFOIL

[Slopes taken at $\alpha_o = 0^\circ$ and $\delta_f = 0^\circ$]

Parameter	Plain overhang		$0.35c_f$ overhang				$0.50c_f$ overhang			
			Blunt nose		Elliptical nose		Blunt nose		Elliptical nose	
	Gap sealed	Gap 0.005c	Gap sealed	Gap 0.005c	Gap sealed	Gap 0.005c	Gap sealed	Gap 0.005c	Gap sealed	Gap 0.005c
$\left(\frac{\partial c_l}{\partial \alpha_o}\right)_{\delta_f,\delta_t}$	0.102	0.096	0.096	0.087	0.097	0.086	0.100	0.090	0.098	0.086
$\left(\frac{\partial c_l}{\partial \delta_f}\right)_{\alpha_o,\delta_t}$	.052	.042	.044	.043	.047	.032	.046	.049	.040	.030
$\left(\frac{\partial \alpha_o}{\partial \delta_f}\right)_{c_l,\delta_t}$	-.51	-.44	-.46	-.49	-.48	-.37	-.46	-.54	-.40	-.34
$\left(\frac{\partial c_{h_f}}{\partial \alpha_o}\right)_{\delta_f,\delta_t}$	-.0050	-.0025	-.0022	-.0006	-.0046	-.0008	.0017	.0039	.0012	.0048
$\left(\frac{\partial c_{h_f}}{\partial \delta_f}\right)_{\alpha_o,\delta_t}$	-.0122	-.0097	-.0020	-.0022	-.0044	-.0023	.0026	.0064	-.0012	-.0012
$\left(\frac{\partial c_m}{\partial c_l}\right)_{\delta_f,\delta_t}$	0	.0135	.0104	.0230	.0103	.0232	.0070	.0167	.0133	.0186
$\left(\frac{\partial c_m}{\partial c_l}\right)_{\alpha_o,\delta_t}$	-.206	-.207	-.200	-.192	-.194	-.223	-.191	-.176	-.210	-.247

NATIONAL ADVISORY
COMMITTEE FOR AERONAUTICS

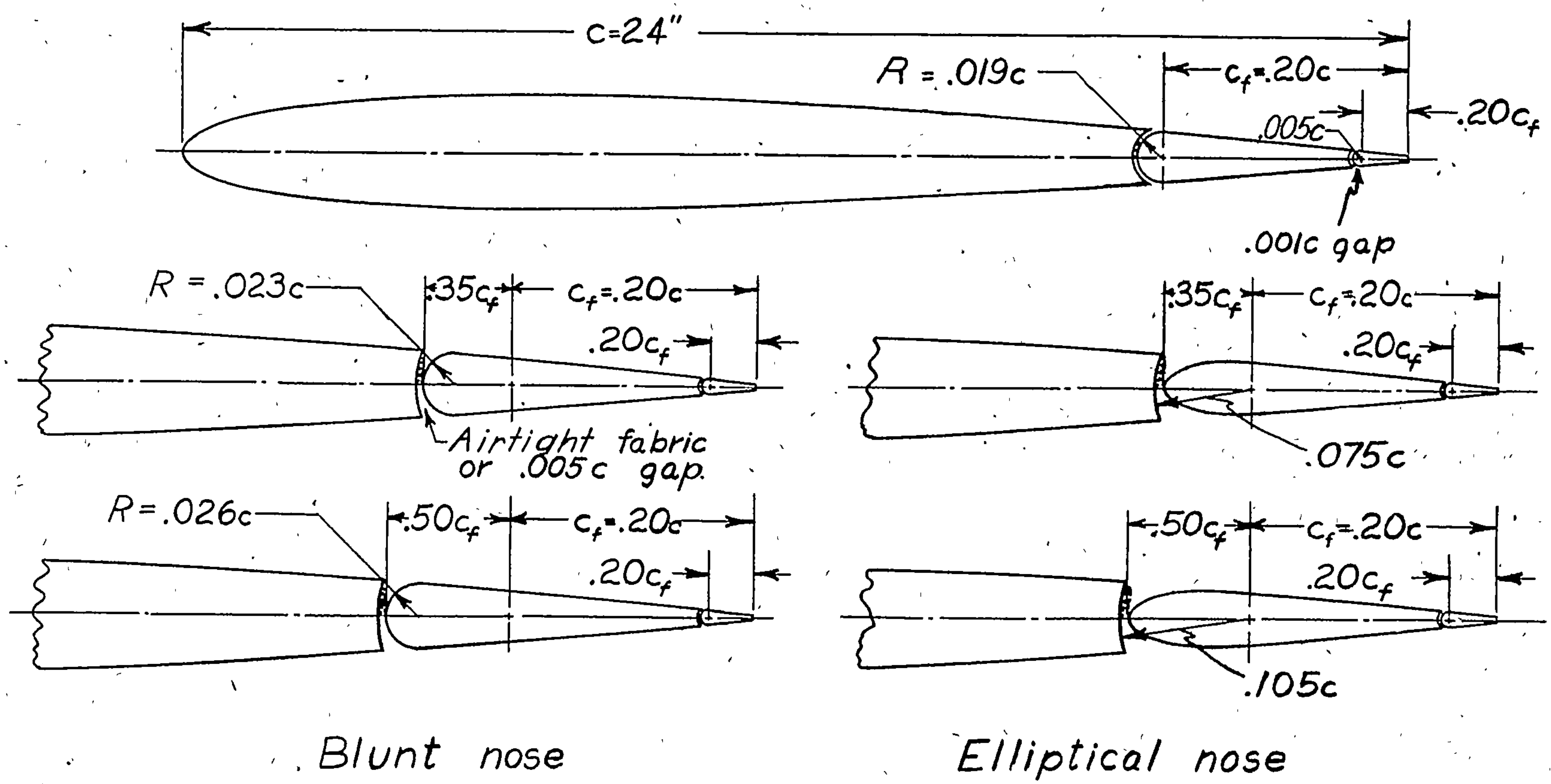

Figure 1.- Nose shapes tested on 0.20c flap with 0.35c_f and 0.50c_f blunt-nose and elliptical-nose overhangs on NACA 0009 airfoil. (For ordinates of elliptical-nose overhang, see table II.)

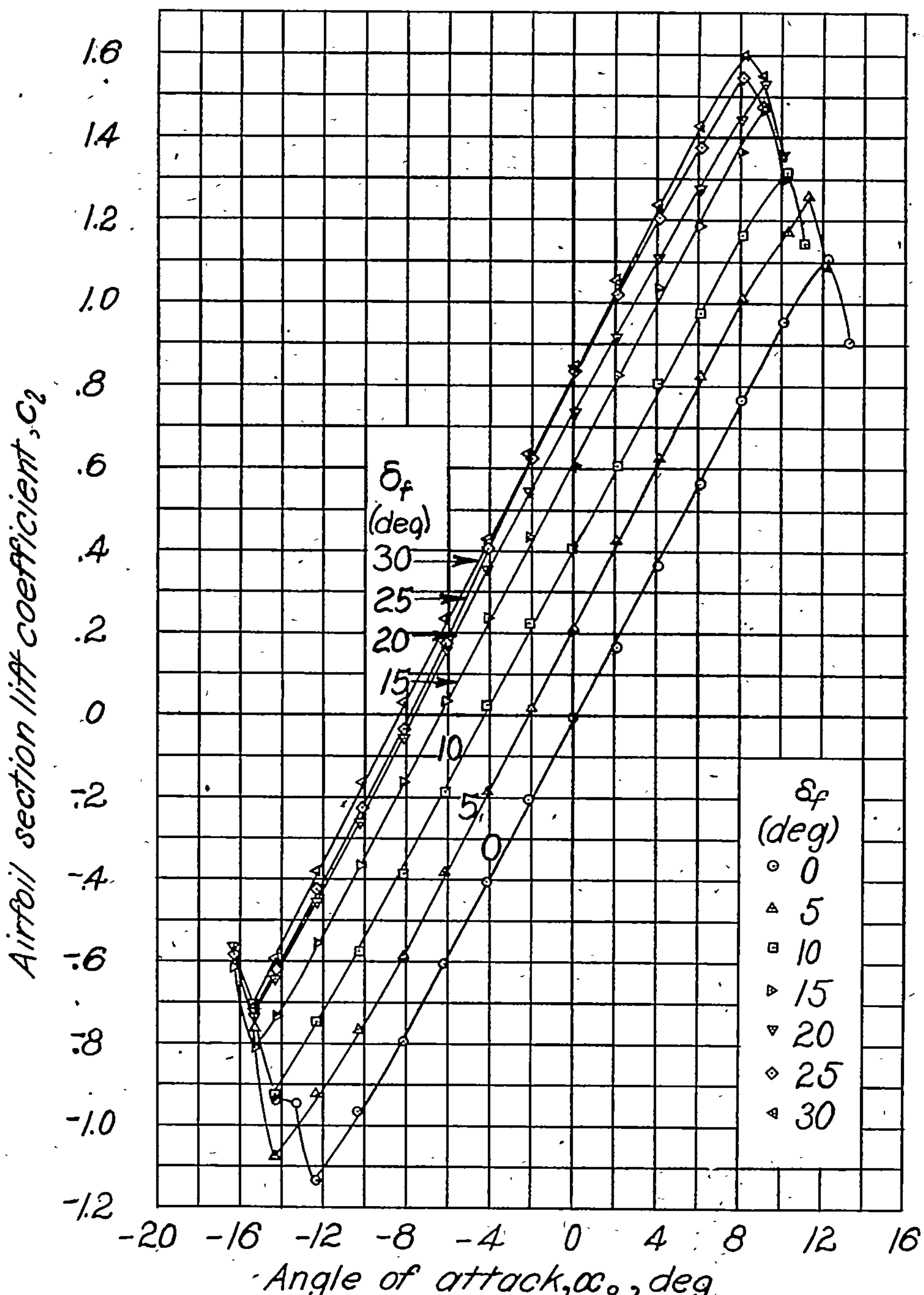

Figure 2.- Aerodynamic section characteristics of an NACA 0009 airfoil with a 0.20c plain flap. Flap gap, 0.005c; tab, 0.20c_f; tab gap, 0.001c; $\delta_t = 0°$.

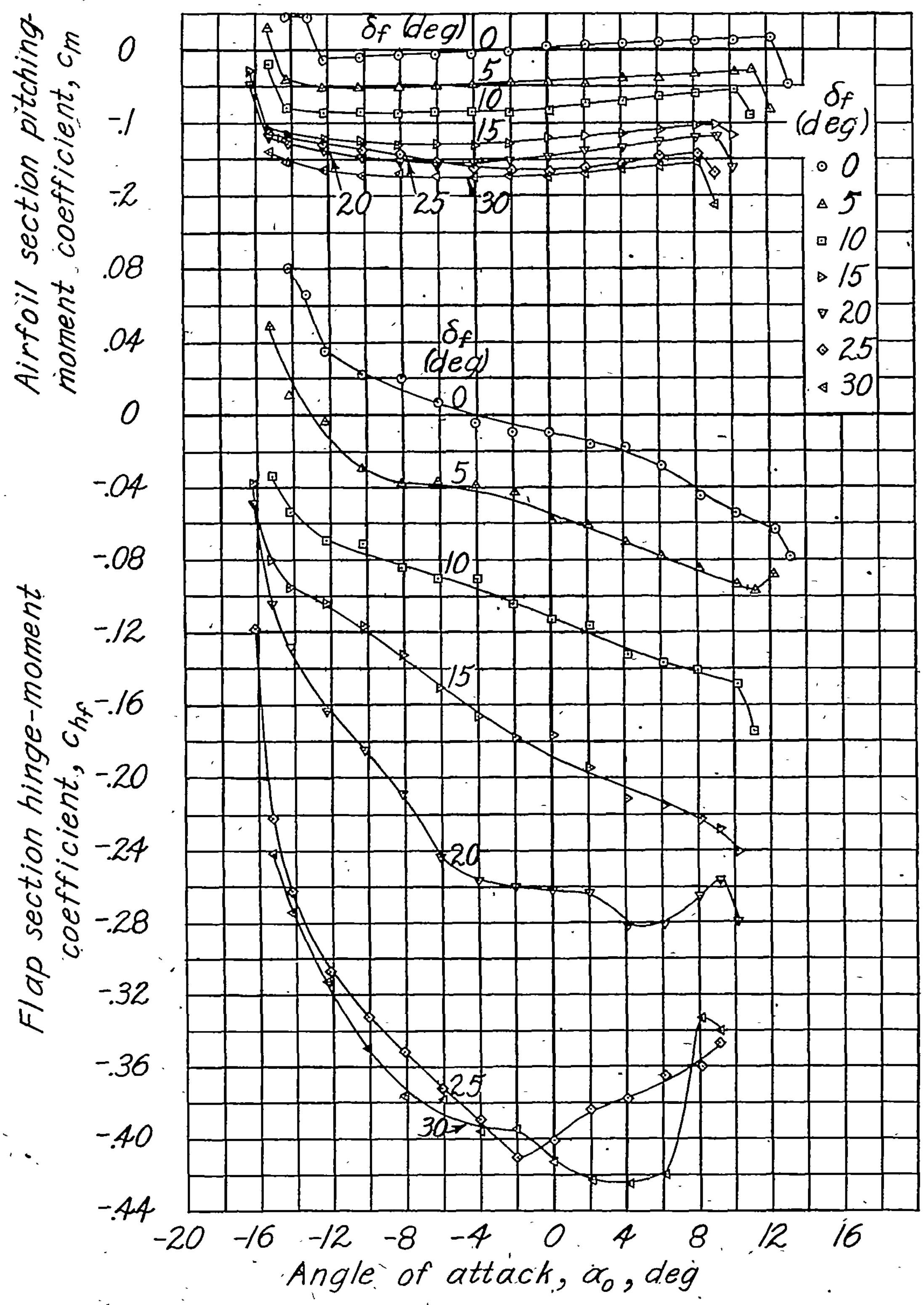

Figure 2 .- Concluded.

NATIONAL ADVISORY
COMMITTEE FOR AERONAUTICS

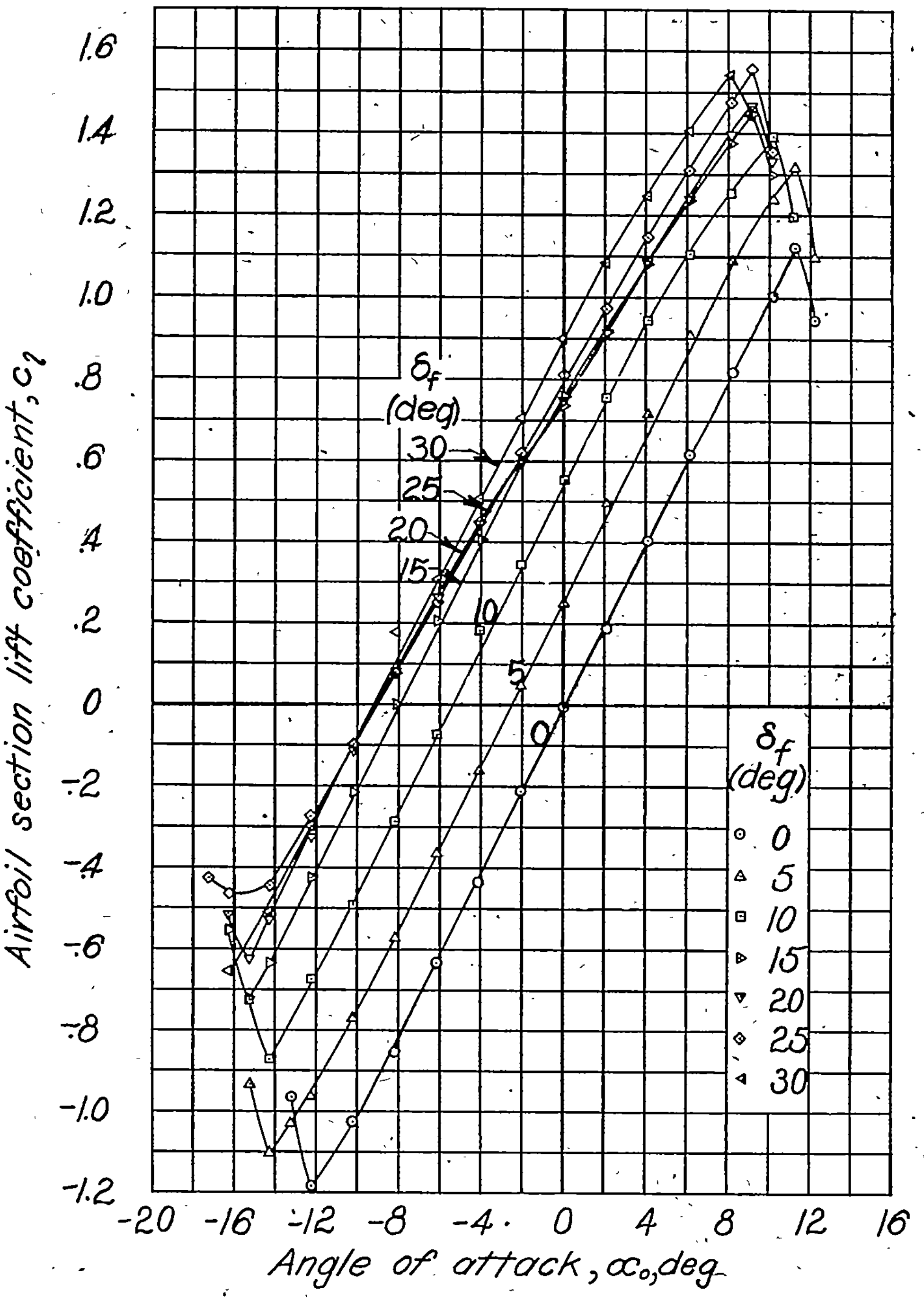

Figure 3.- Aerodynamic section characteristics of an NACA 0009 airfoil with a 0.20c plain flap. Flap gap sealed; tab, 0.20 c_f; tab gap, 0.001c; $\delta_t = 0°$.

NATIONAL ADVISORY COMMITTEE FOR AERONAUTICS

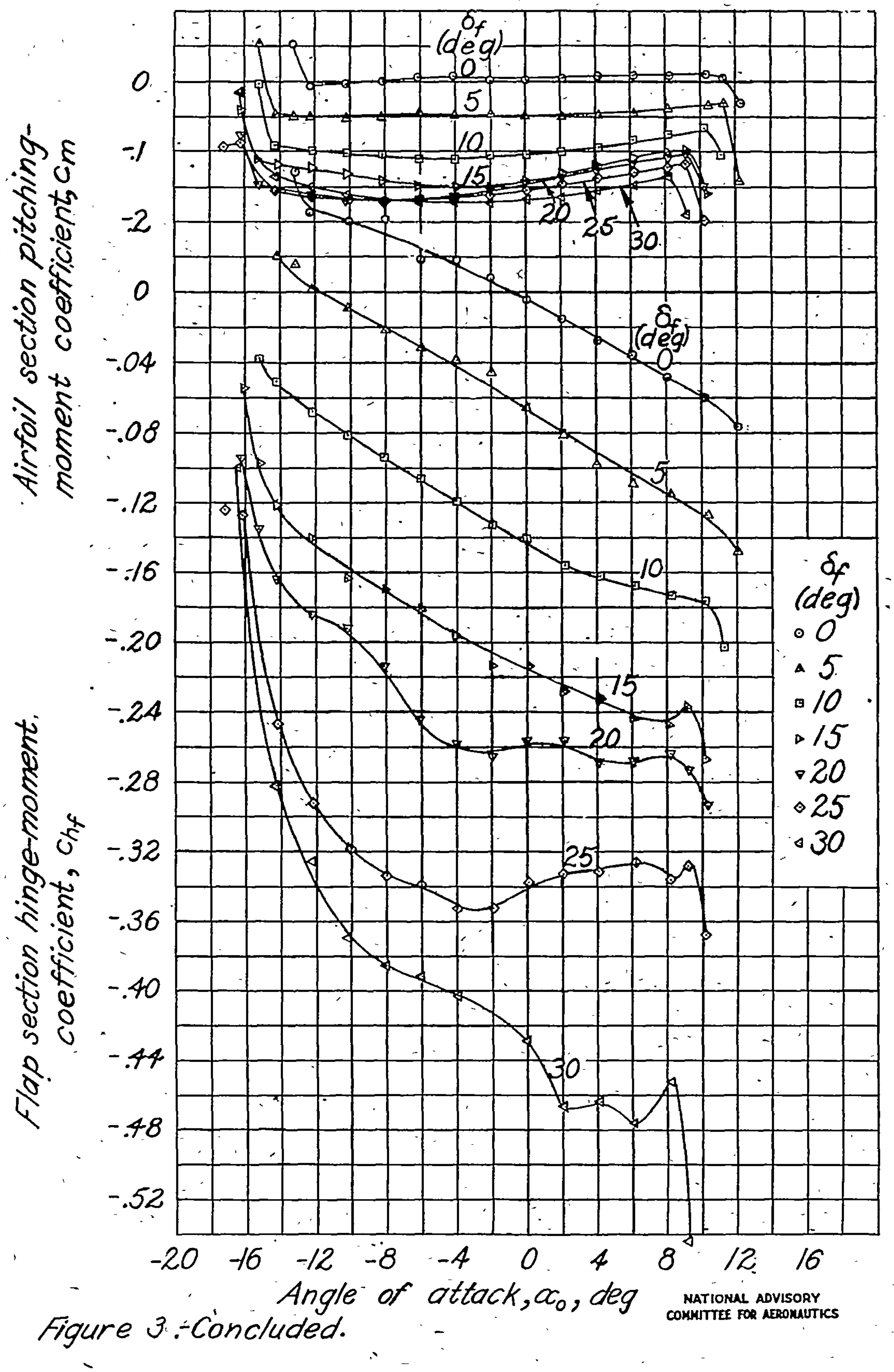

NATIONAL ADVISORY COMMITTEE FOR AERONAUTICS

Figure 3.-Concluded.

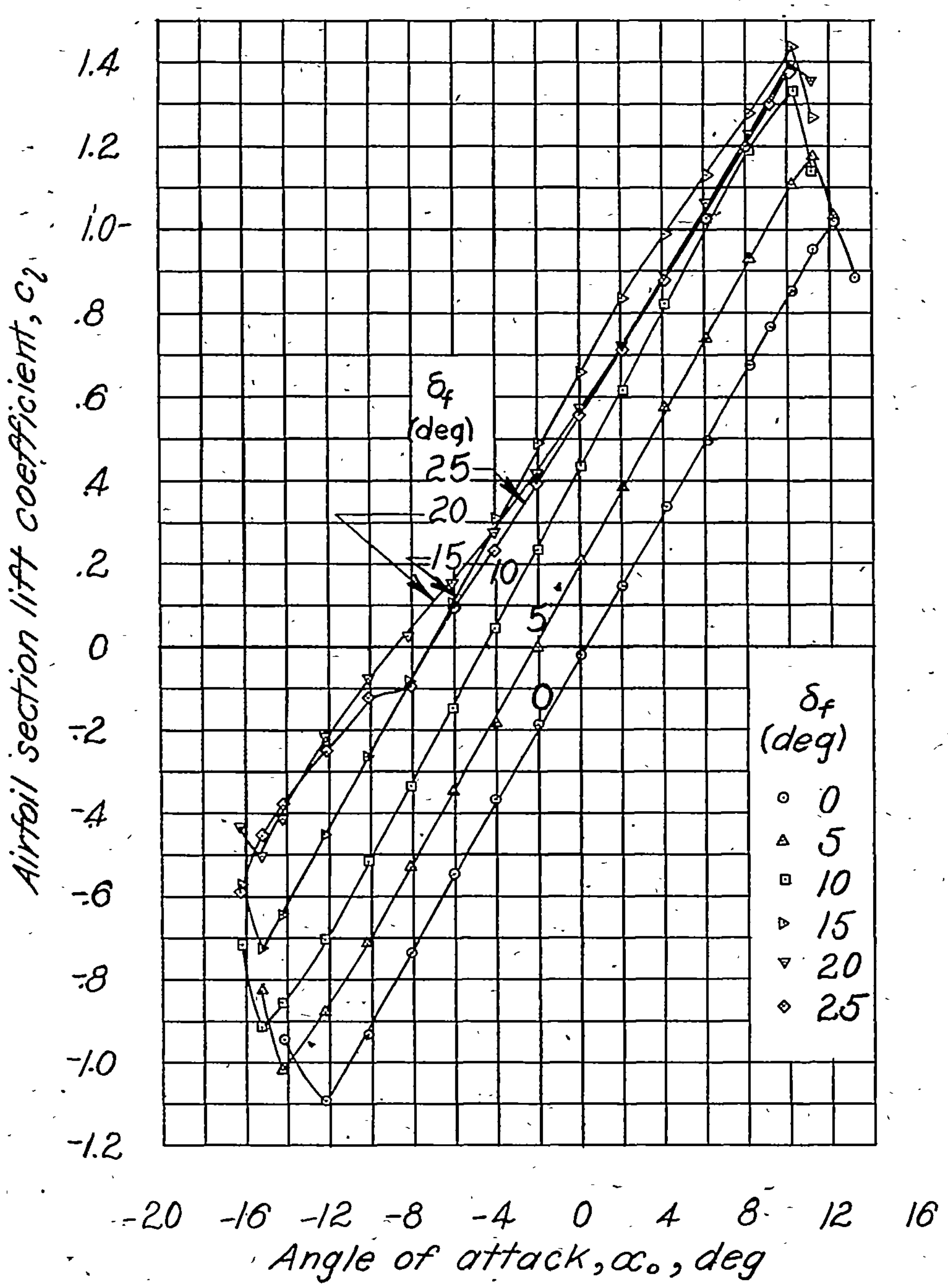

Figure 4.- Aerodynamic section characteristics of an NACA 0009 airfoil with a 0.20c flap having a 0.35c_f overhang with blunt nose. Flap gap, 0.005c; tab, 0.20c_f; tab gap, 0.001c; $\delta_t = 0°$.

NATIONAL ADVISORY
COMMITTEE FOR AERONAUTICS

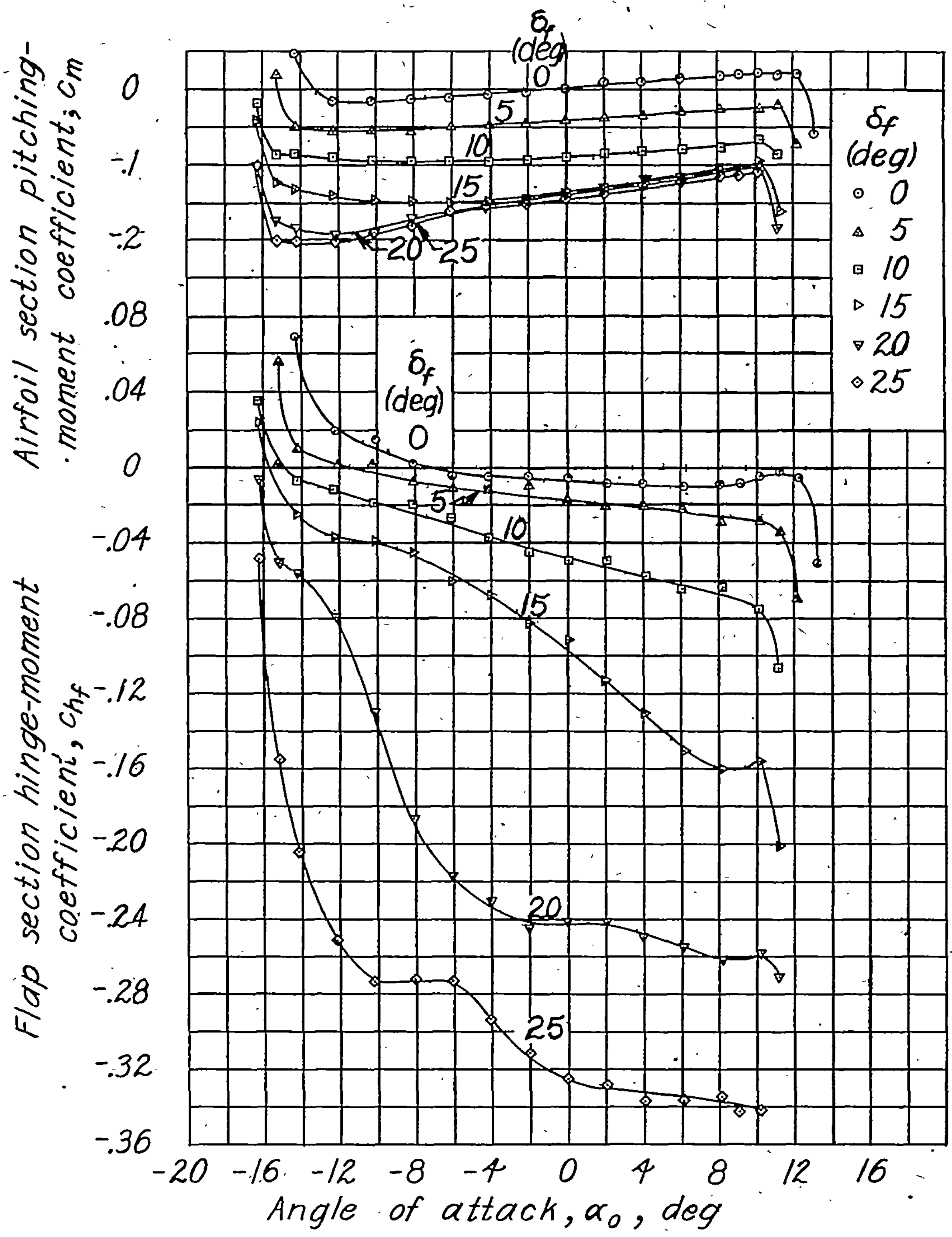

Figure 4.- Concluded.

NATIONAL ADVISORY COMMITTEE FOR AERONAUTICS

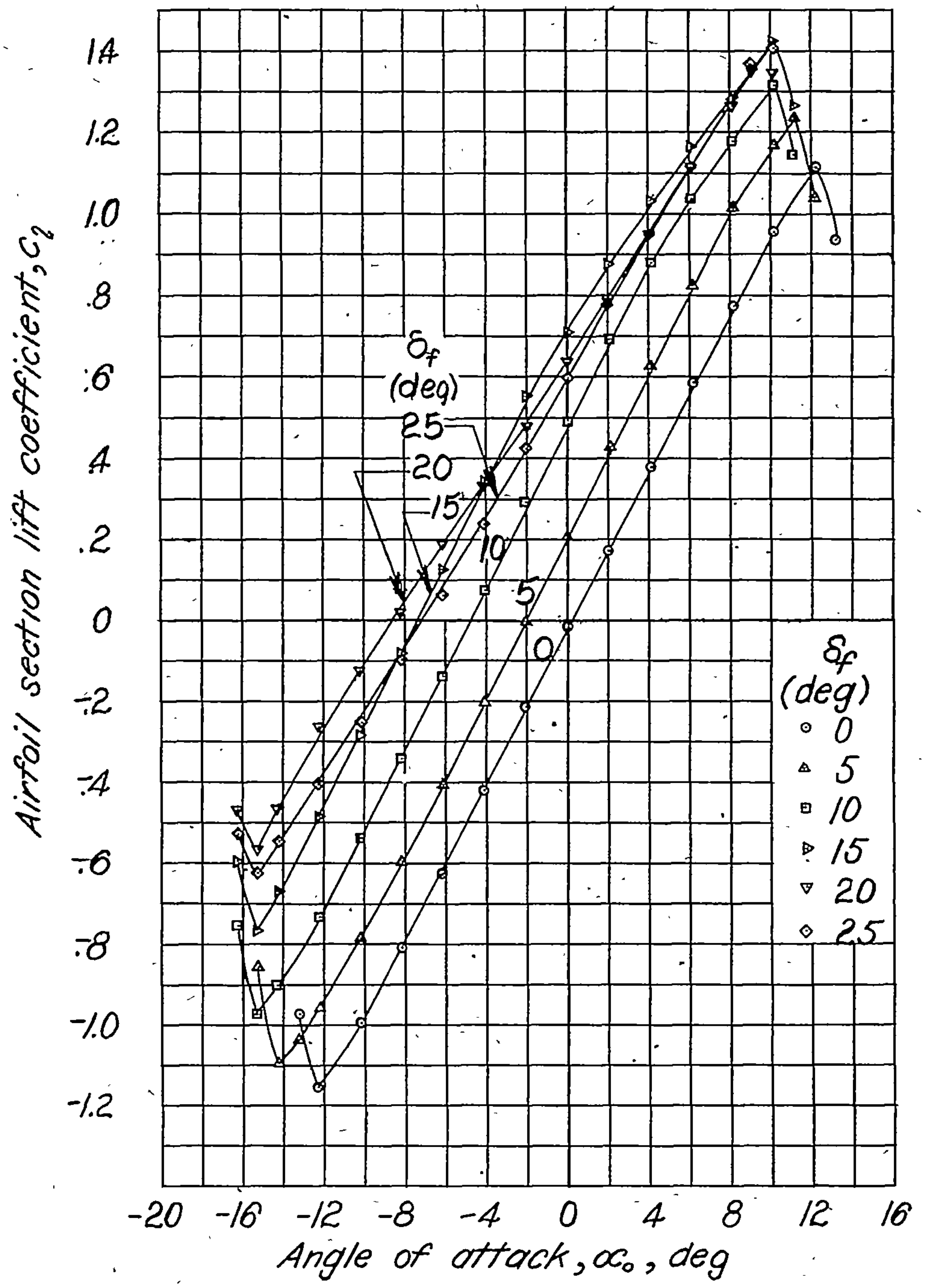

Figure 5.- Aerodynamic section characteristics of an NACA 0009 airfoil with a 0.20c flap having a 0.35c_f overhang with blunt nose. Flap gap, sealed; tab, 0.20c_f; tab gap, 0.001c ; $\delta_t = 0°$.

NATIONAL ADVISORY COMMITTEE FOR AERONAUTICS

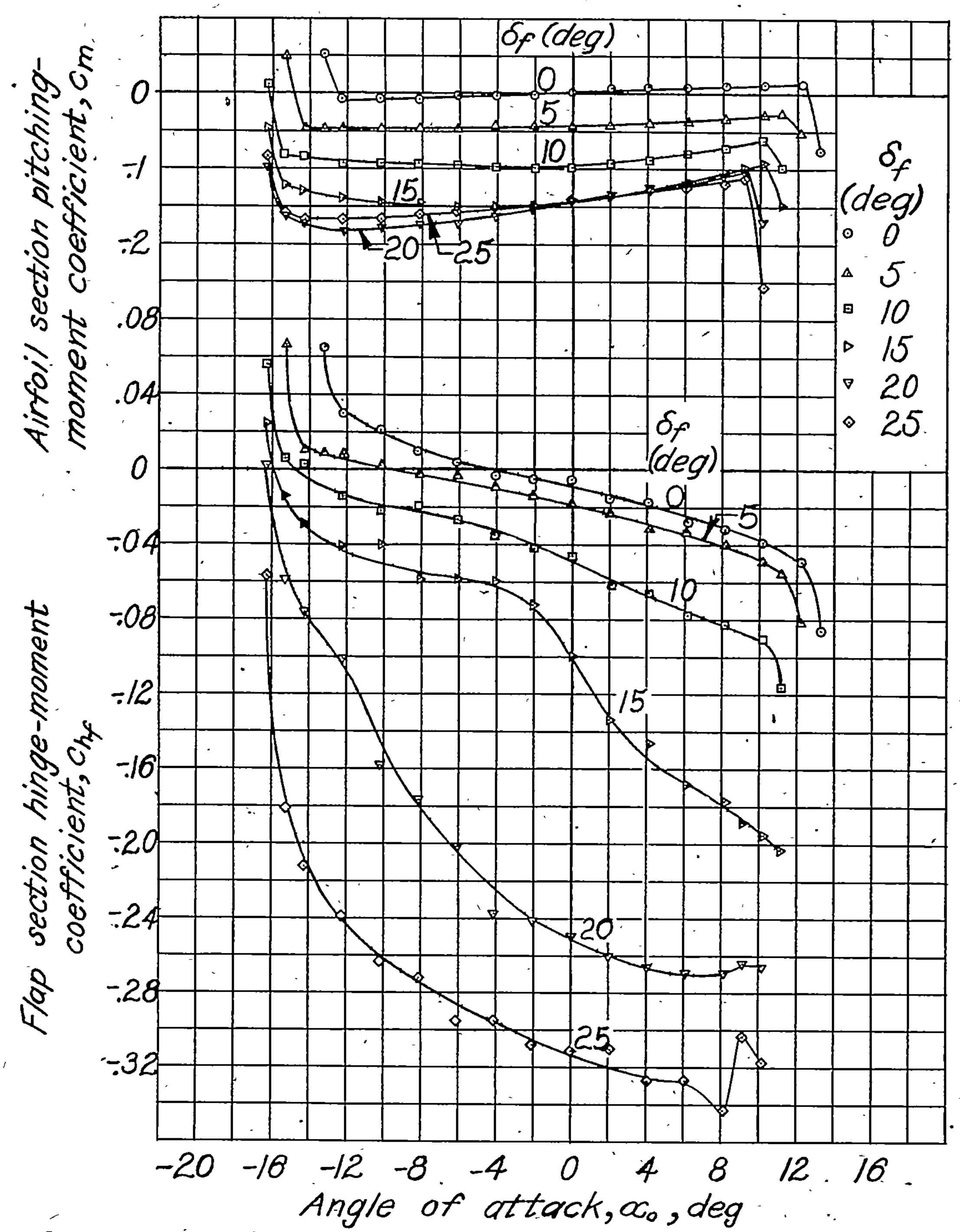

Figure 5.- Concluded.

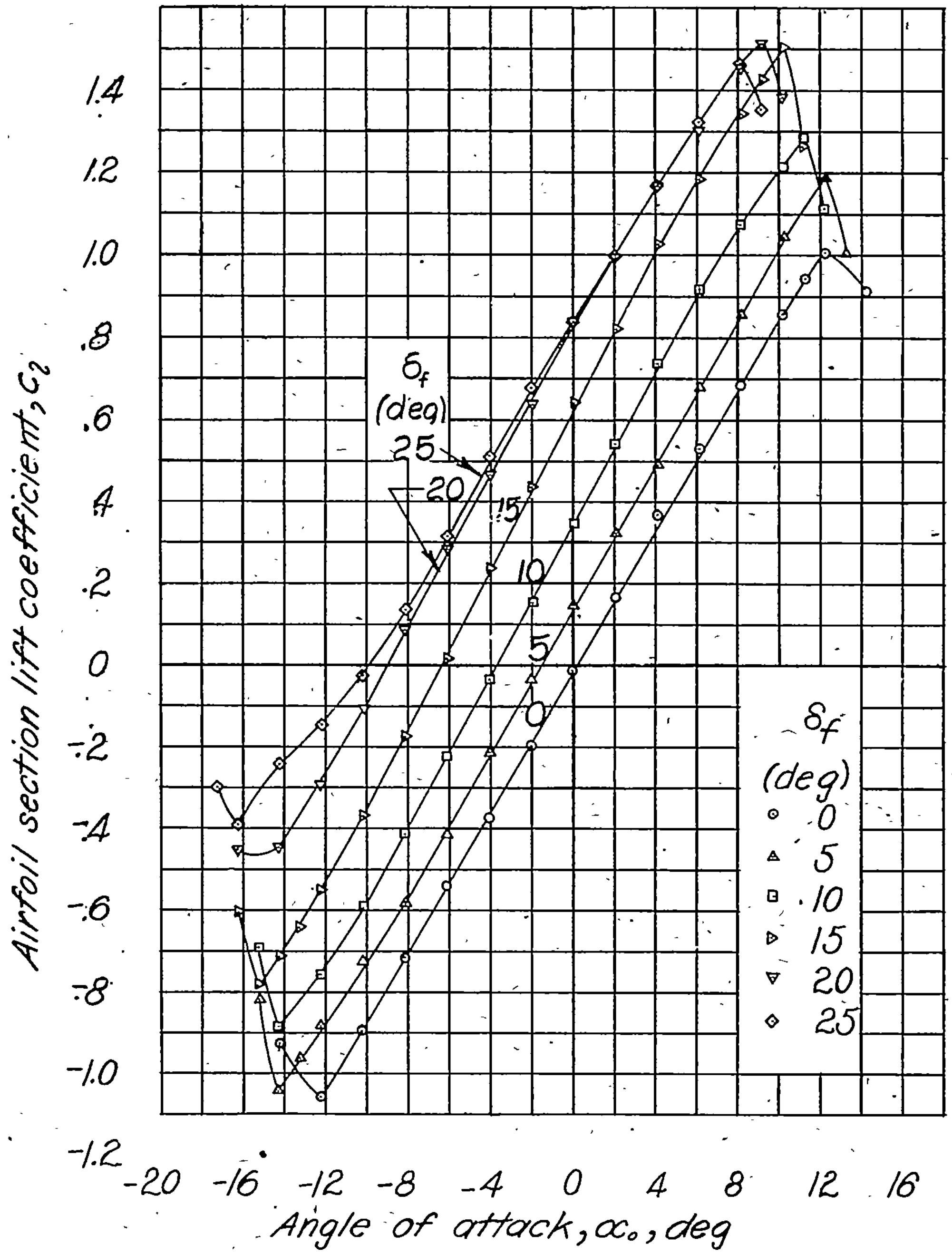

Figure 6.-Aerodynamic section characteristics of an NACA 0009 airfoil with 0.20c flap having a 0.35c_f overhang with elliptical nose. Flap gap, 0.005c; tab, 0.20c_f; tab gap, 0.001c; $\delta_t = 0°$.

NATIONAL ADVISORY COMMITTEE FOR AERONAUTICS

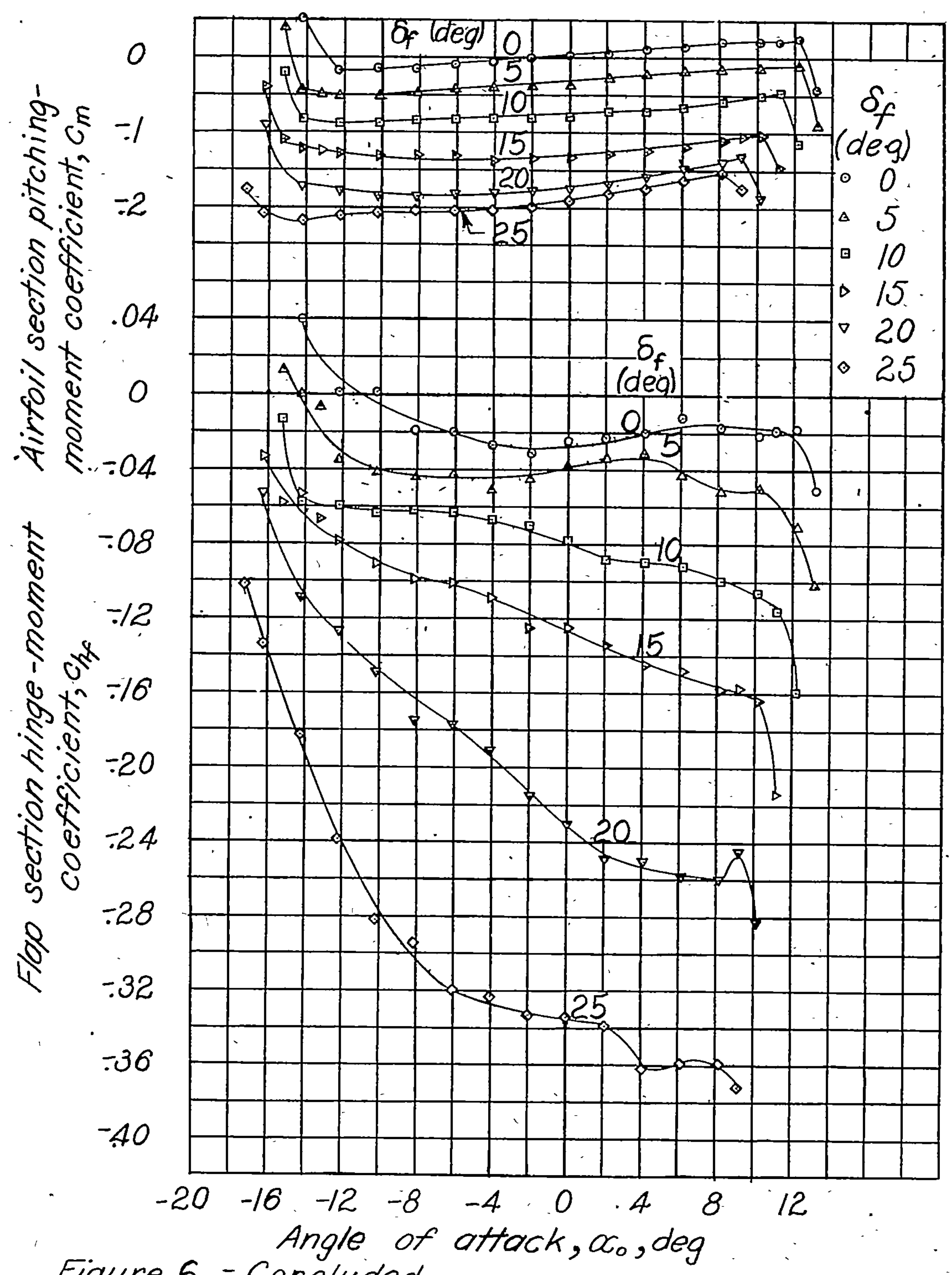

Figure 6 - Concluded.

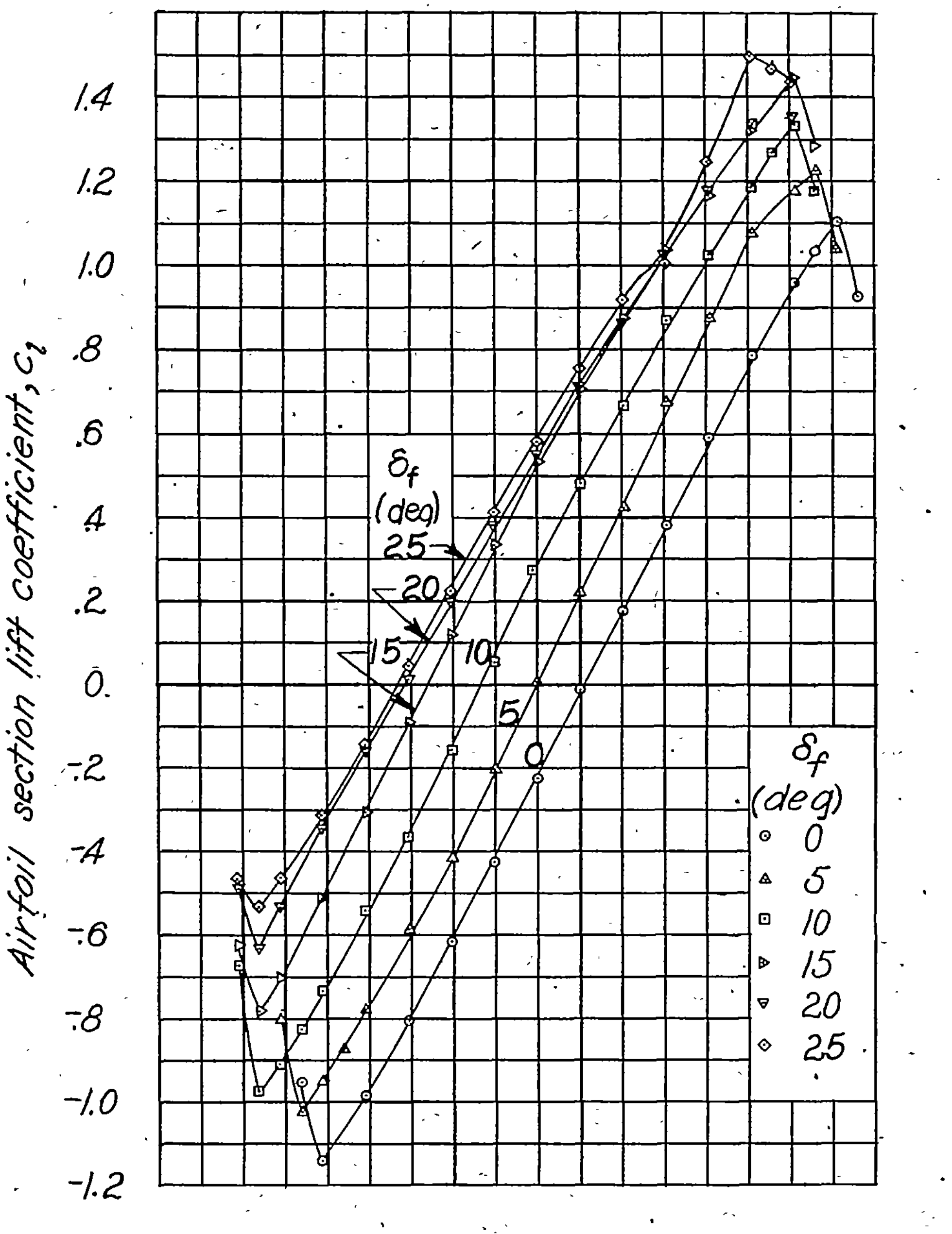

Figure 7.- Aerodynamic section characteristics of an NACA 0009 airfoil with a 0.20c flap having a 0.35c_f overhang with elliptical nose. Flap gap sealed; tab, 0.20c_f; tab gap, 0.001c; $\delta_t = 0°$.

NATIONAL ADVISORY COMMITTEE FOR AERONAUTICS

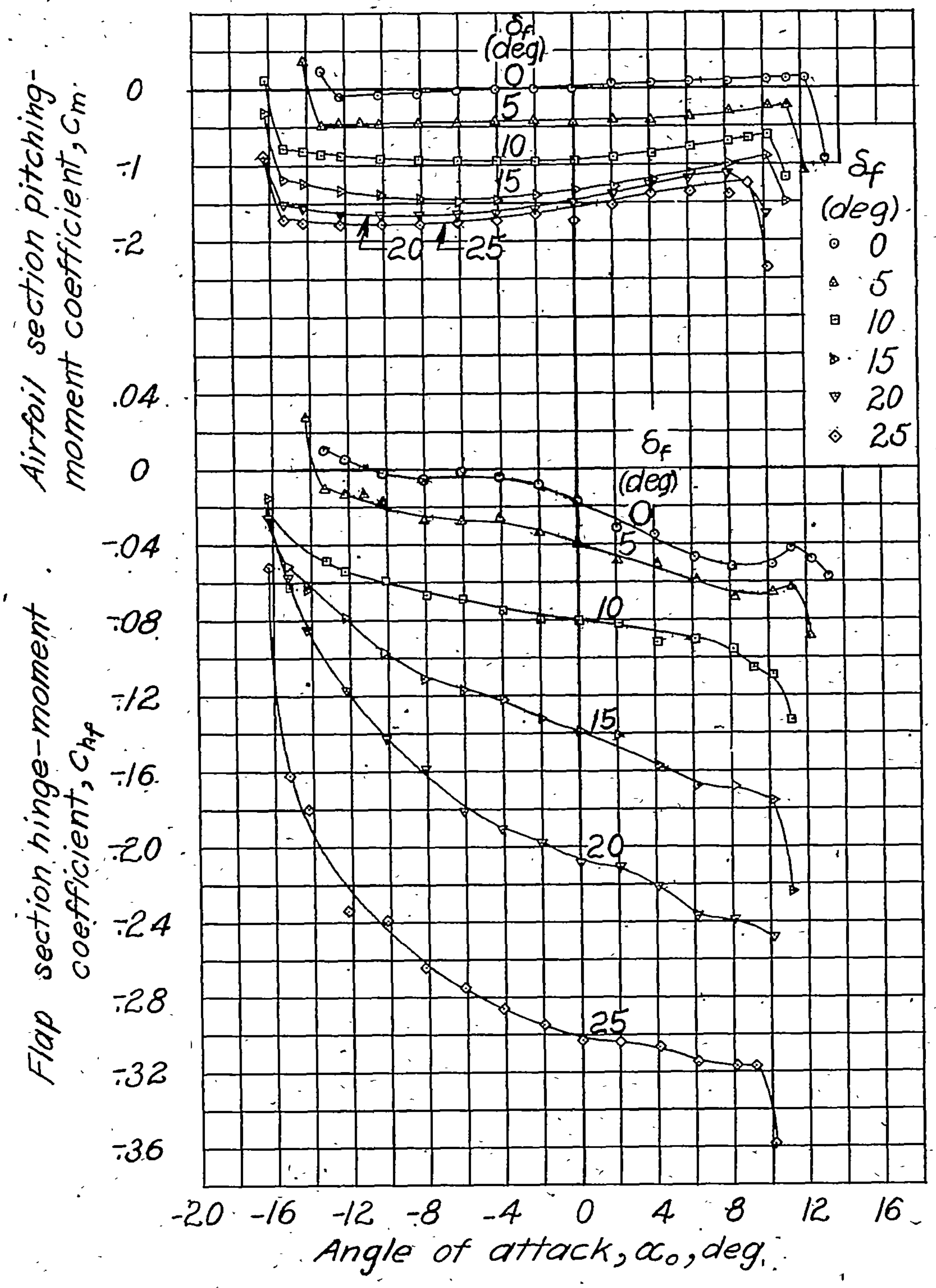

Figure 7. - Concluded.

NATIONAL ADVISORY COMMITTEE FOR AERONAUTICS

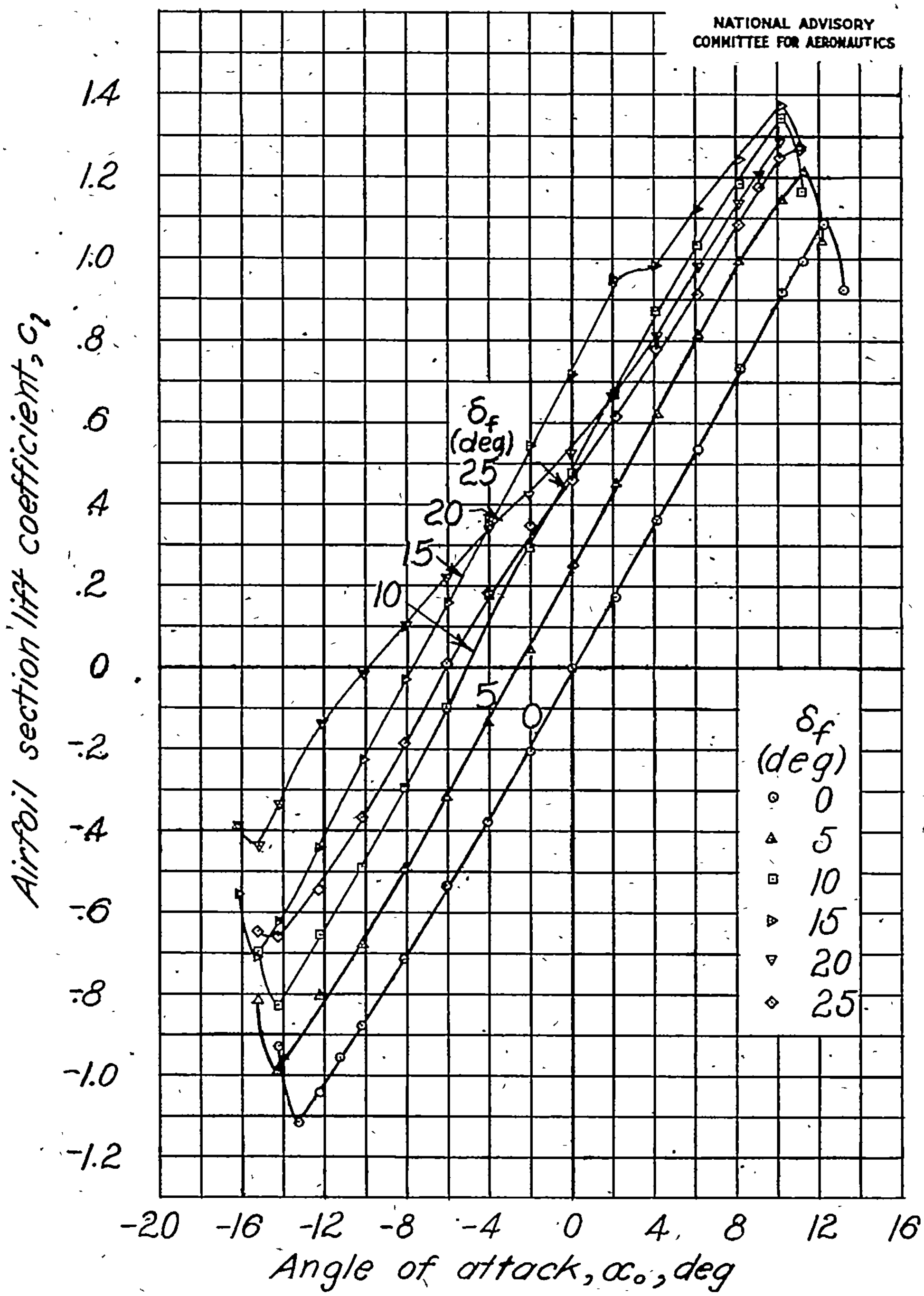

Figure 8.- Aerodynamic section characteristics of an NACA 0009 airfoil with a 0.20c flap having a $0.50c_f$ overhang with blunt nose; Flap gap, 0.005c; tab, $0.20c_f$; tab gap, 0.001c; $\delta_t = 0°$.

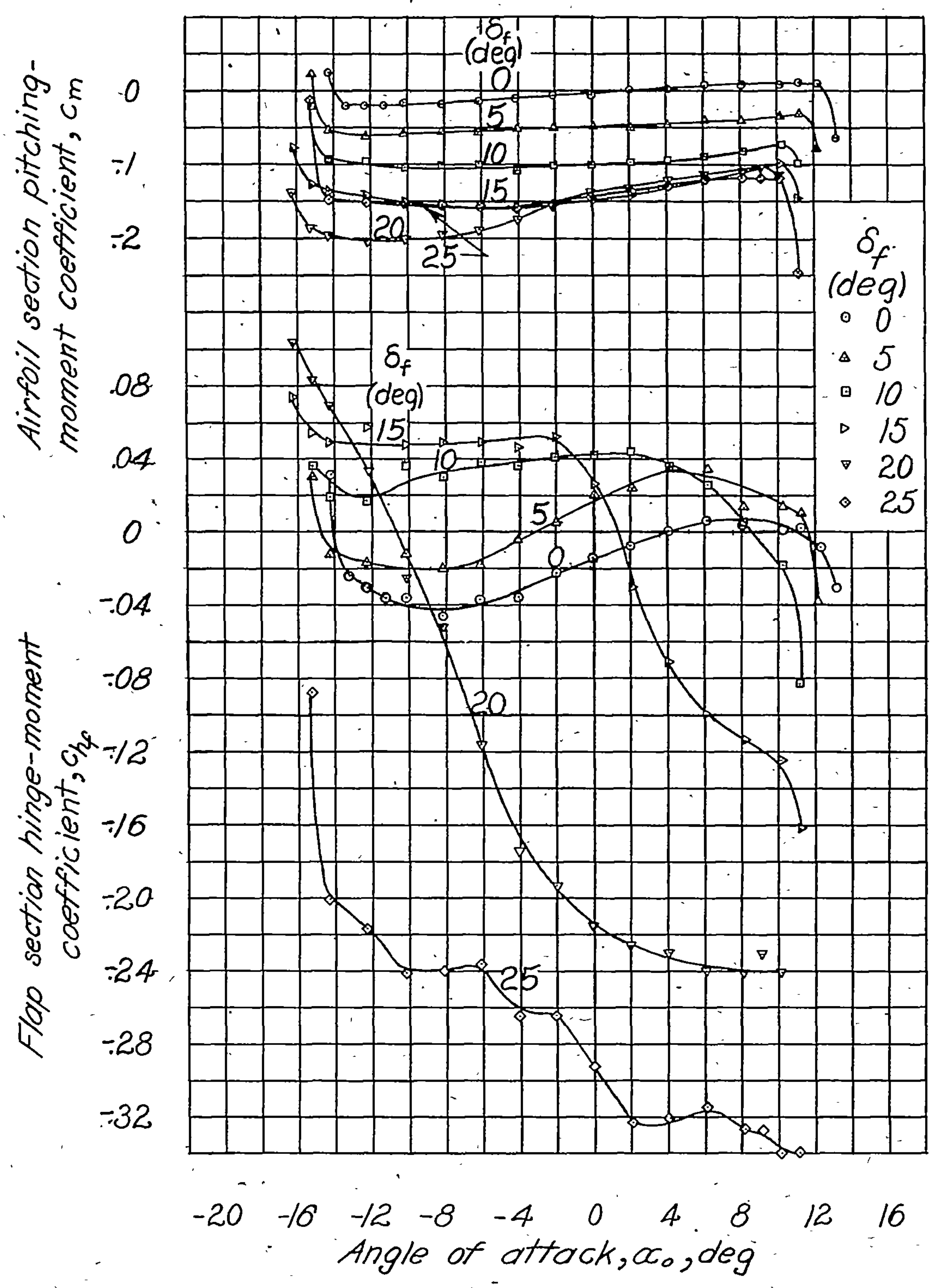

Figure 8 - Concluded.

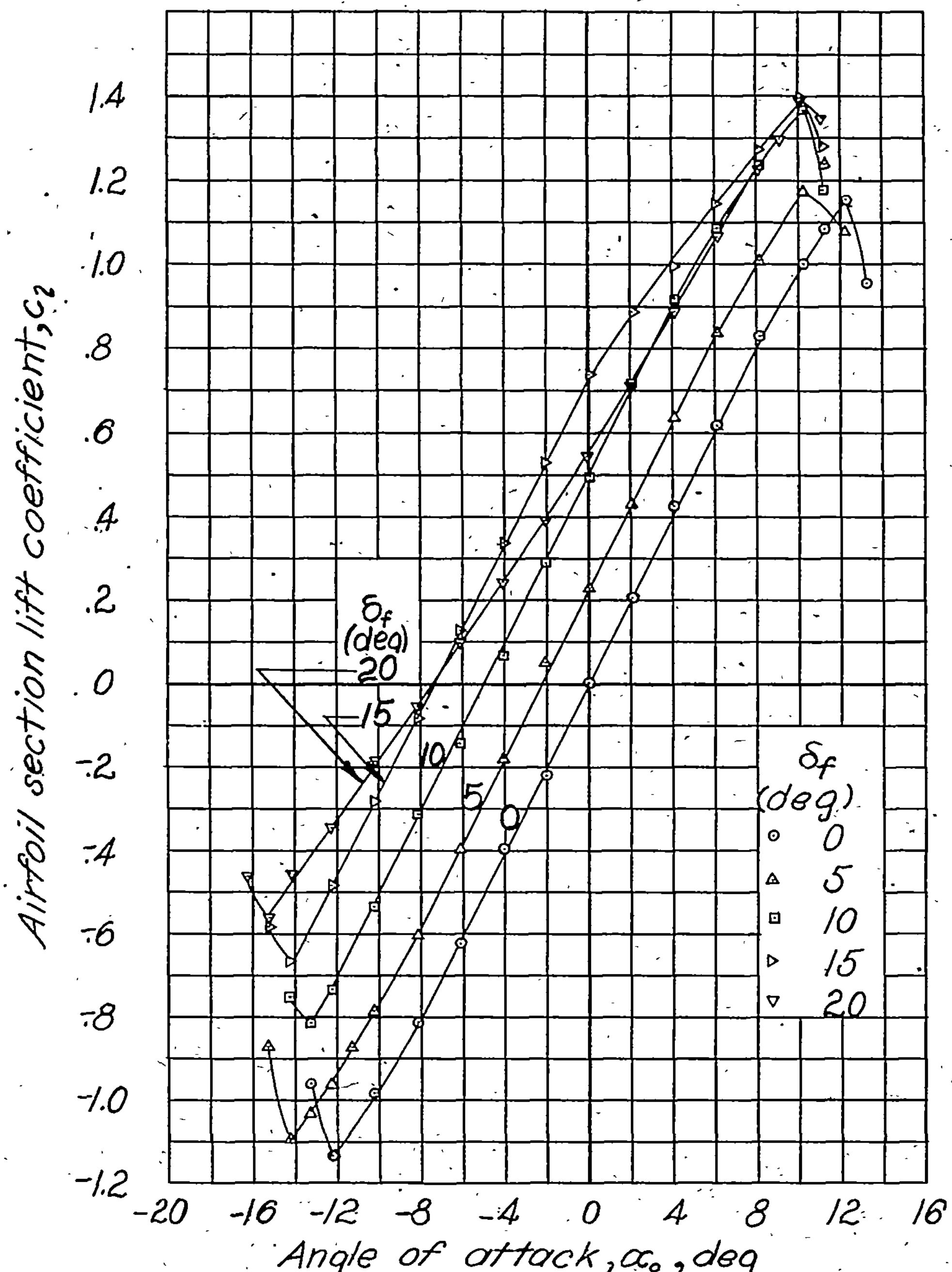

Figure 9.–Aerodynamic section characteristics of an NACA 0009 airfoil with a 0.20c flap having a $0.50c_f$ overhang with blunt nose. Flap gap sealed; tab, $0.20c_f$; tab gap, 0.001c; $\delta_t = 0°$.

NATIONAL ADVISORY
COMMITTEE FOR AERONAUTICS

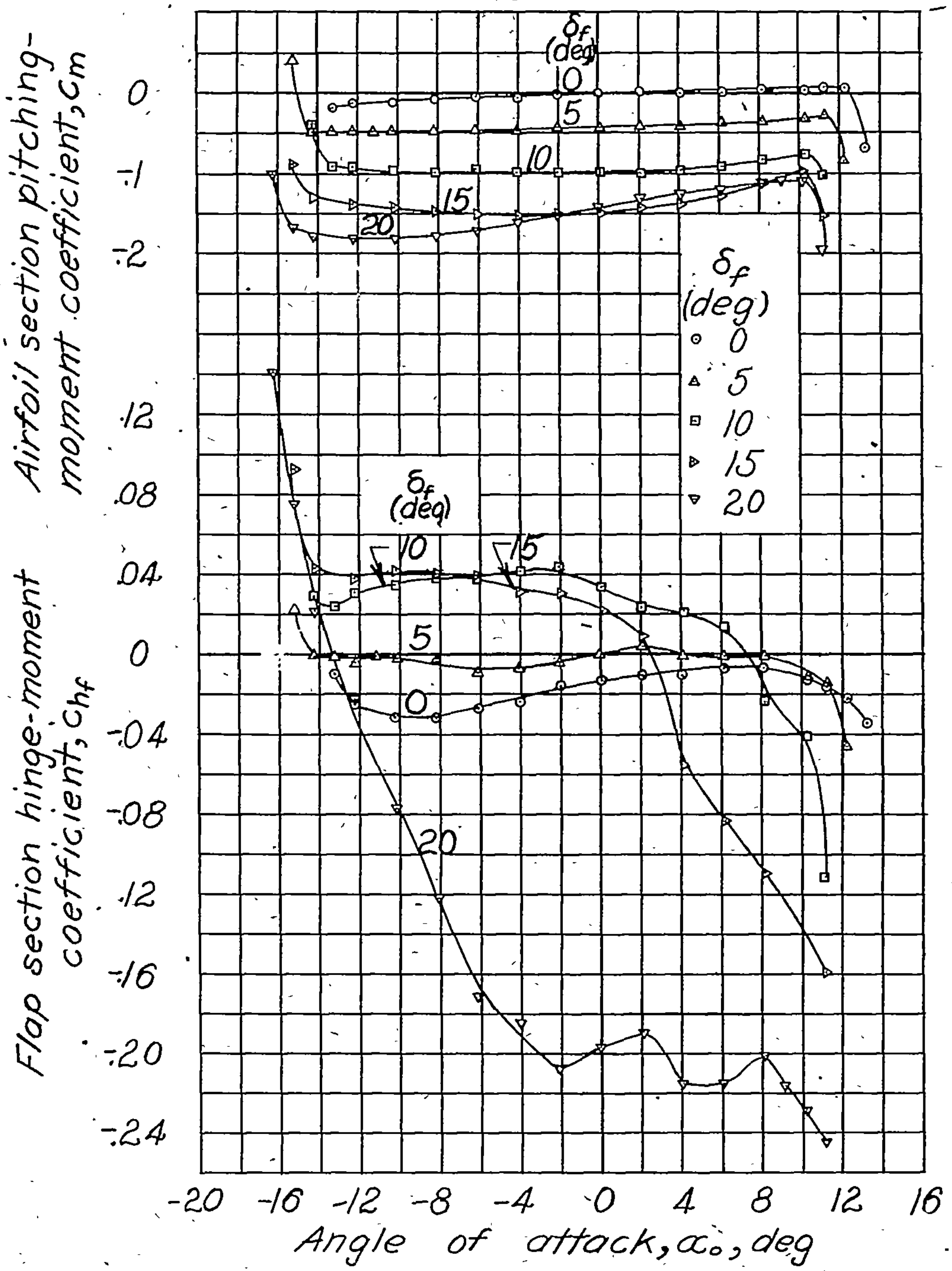

Figure 9.- Concluded.

NATIONAL ADVISORY
COMMITTEE FOR AERONAUTICS

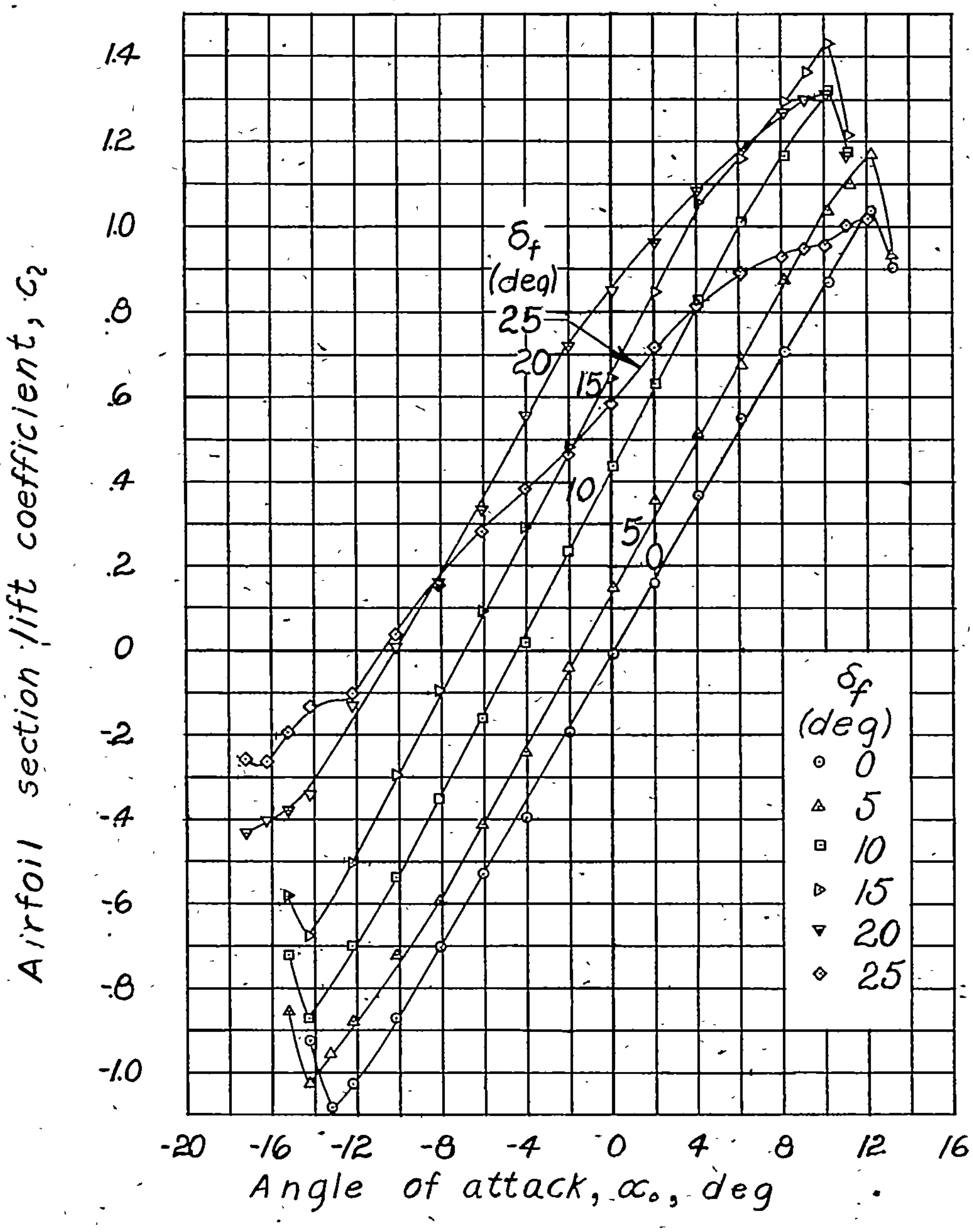

Figure 10. - Aerodynamic section characteristics of an NACA 0009 airfoil with a 0.20c flap having a $0.50c_f$ overhang with elliptical nose. Flap gap, 0.005c; tab, $0.20c_f$; tab gap, 0.001c ; $\delta_t = 0°$.

NATIONAL ADVISORY
COMMITTEE FOR AERONAUTICS

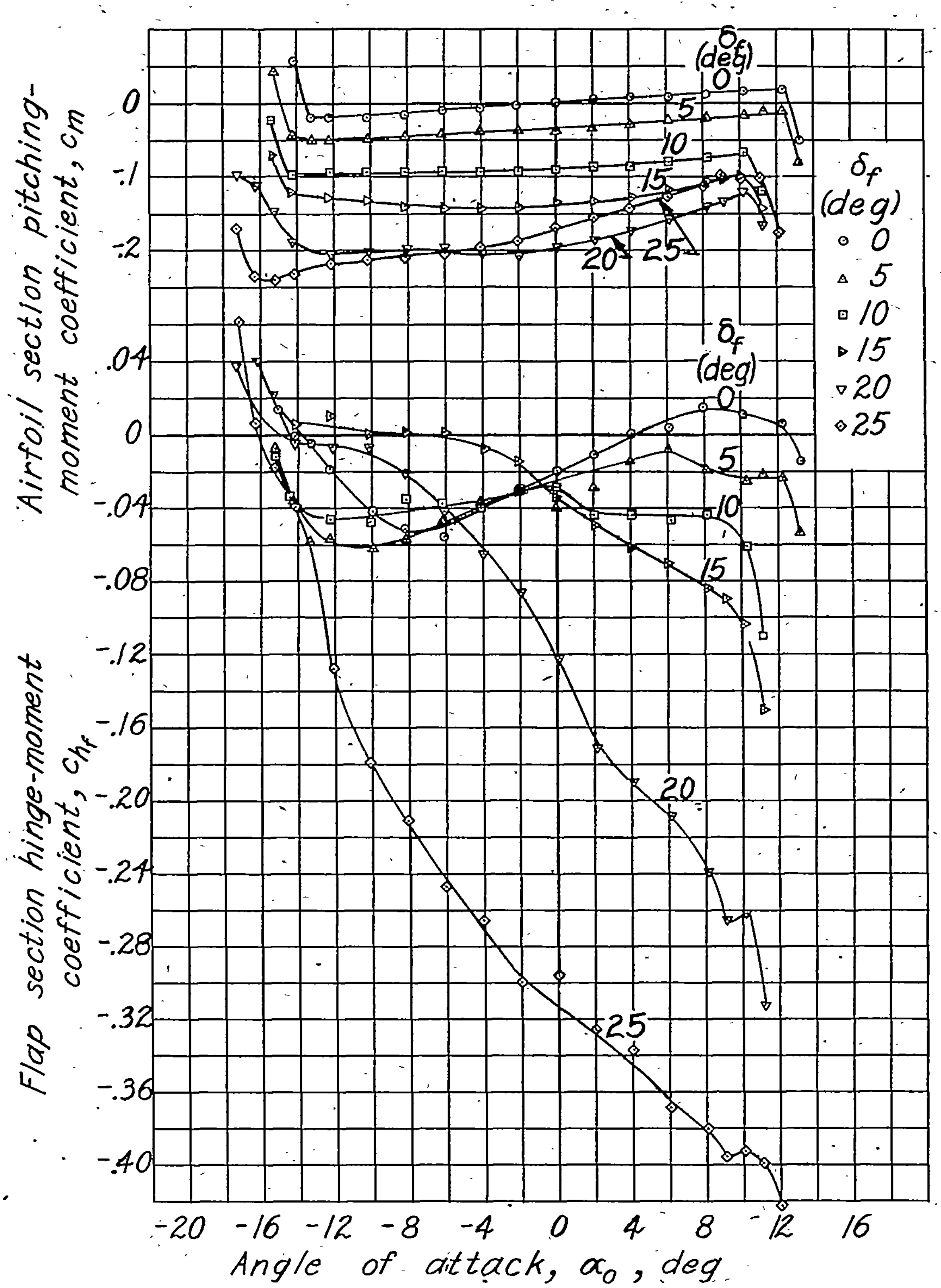

Figure 10.- Concluded.

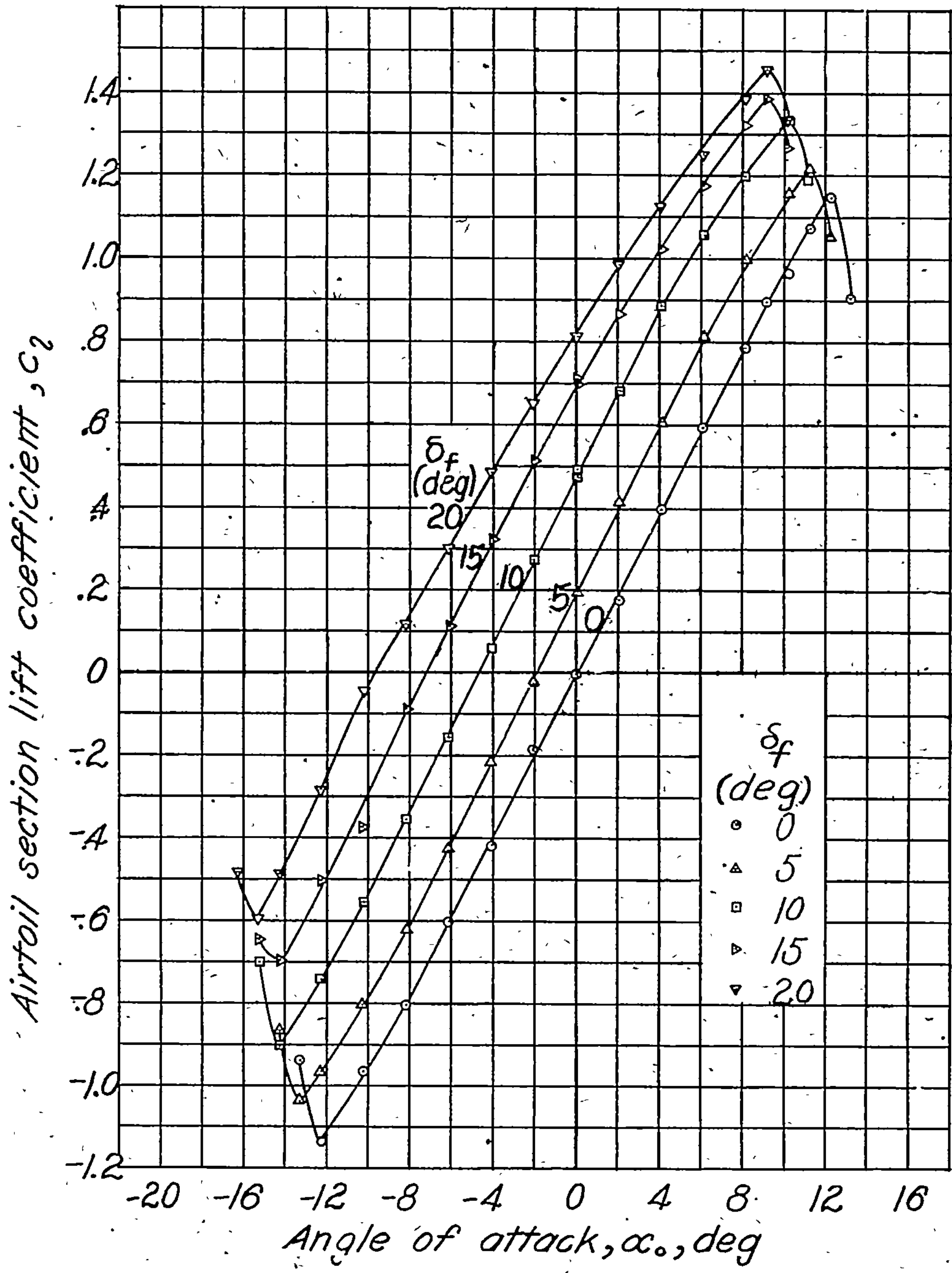

Figure 11. - Aerodynamic section characteristics of an NACA 0009 airfoil with a 0.20c flap having a $0.50c_f$ overhang with elliptical nose. Flap gap sealed; tab, $0.20c_f$; tab gap, 0.001c; $\delta_t = 0°$.

NATIONAL ADVISORY COMMITTEE FOR AERONAUTICS

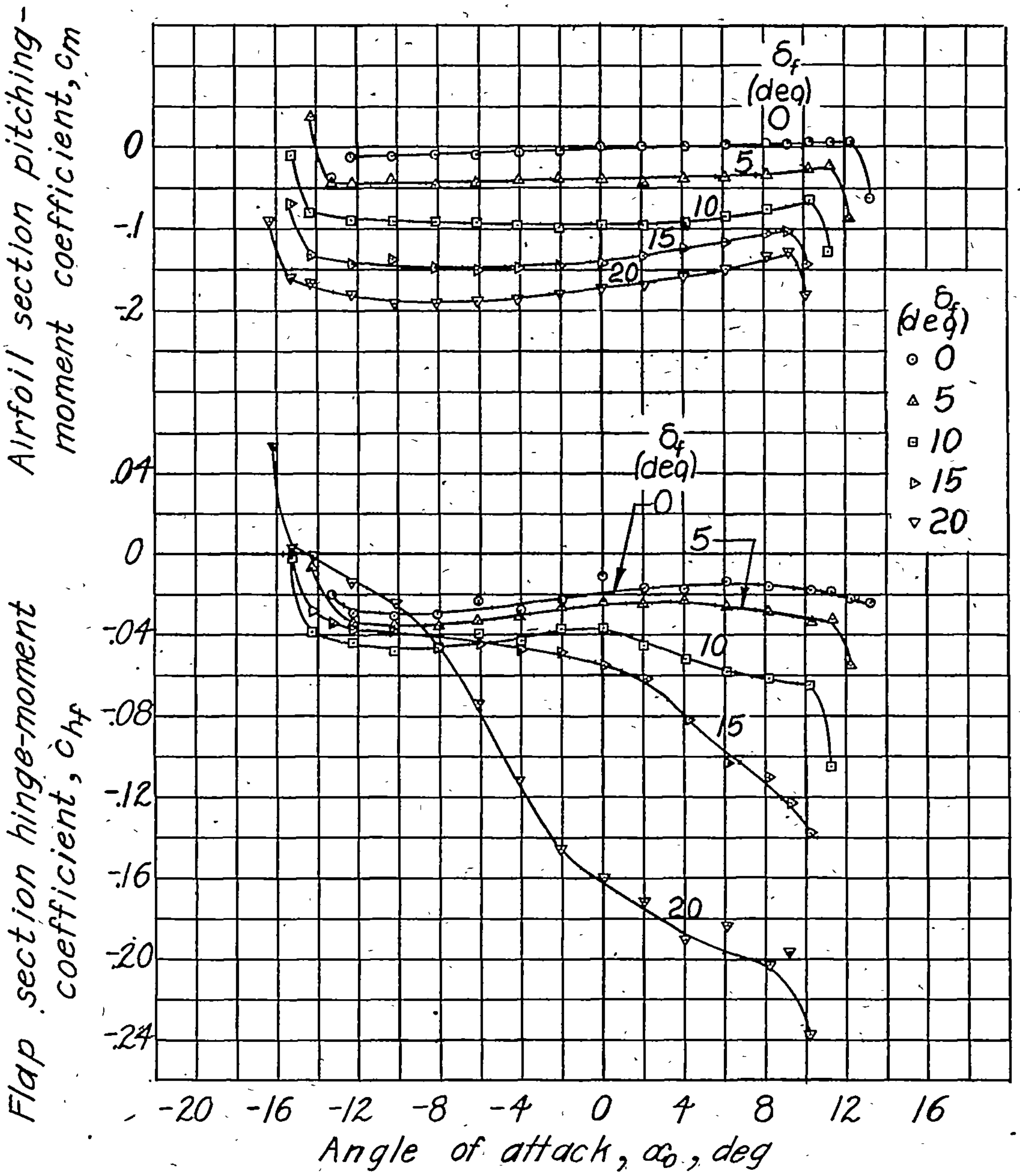

Figure 11.-Concluded.

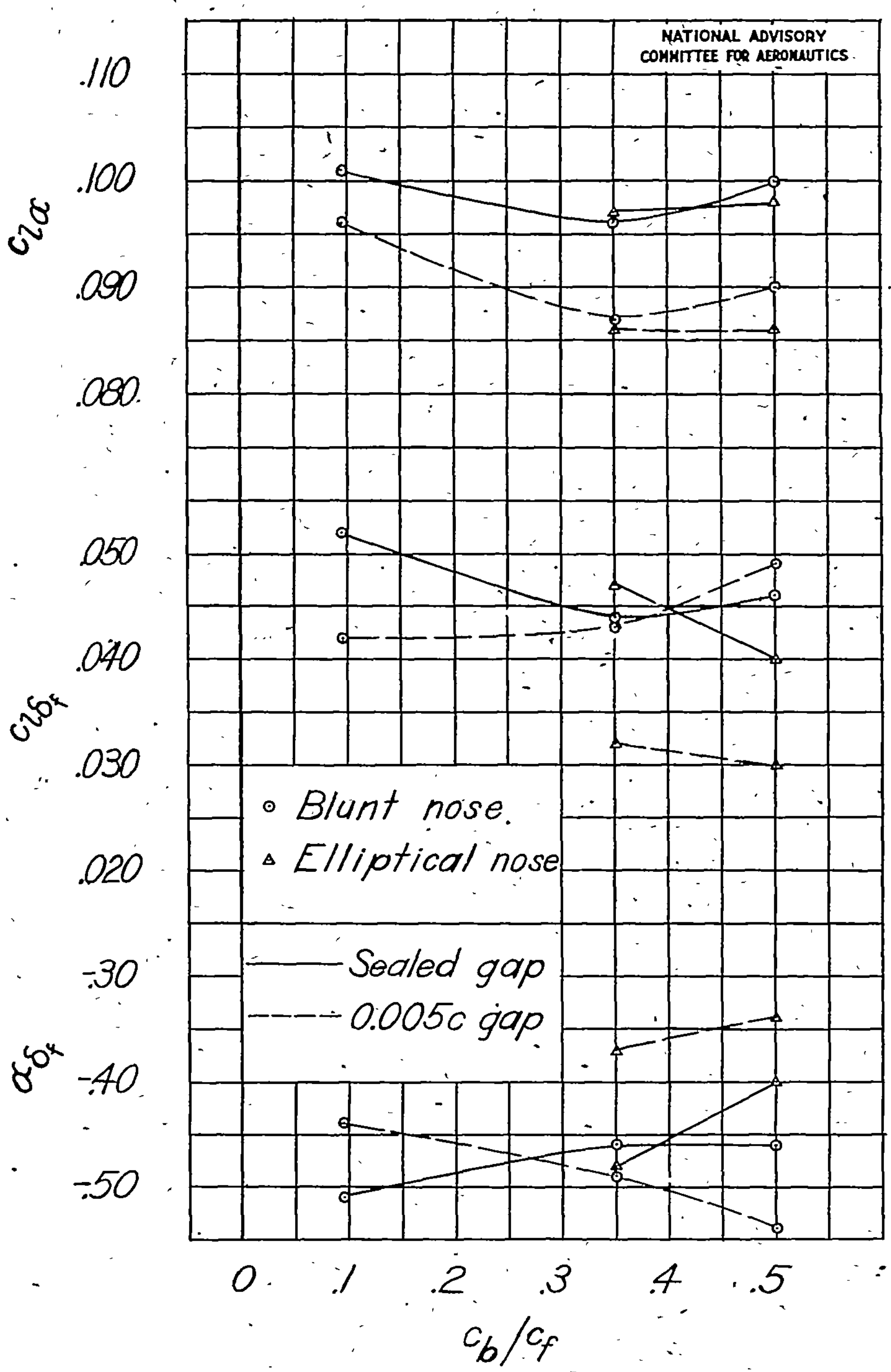

Figure 12 .- Variation of airfoil section lift parameters with overhang on NACA 0009 airfoil. Flap, 0.20c; flap gap, sealed and 0.005c. Tab, 0.20c_f; tab gap, 0.001c; $\delta_t = 0°$.

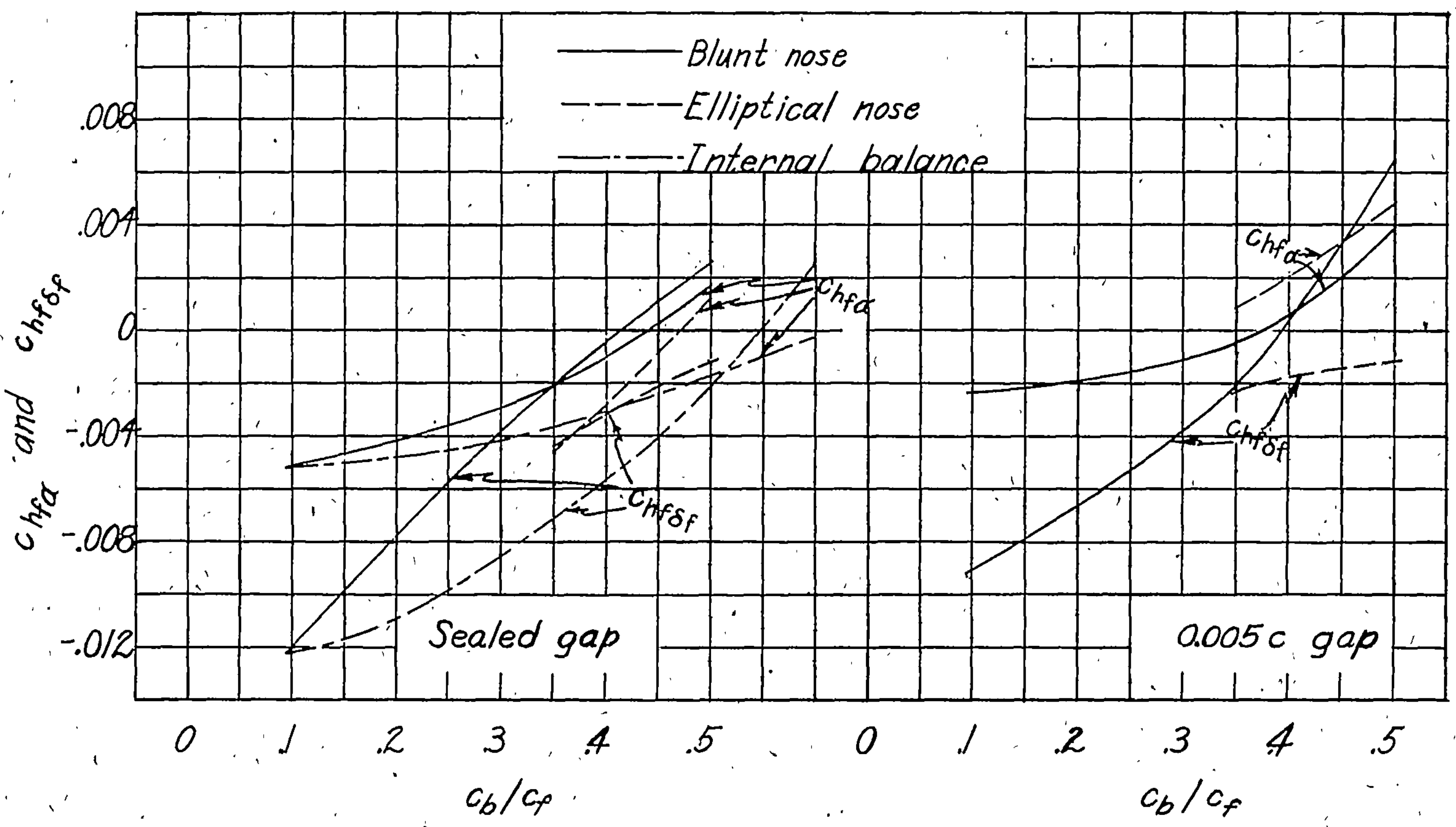

Figure 13.- Variation of flap section hinge-moment parameters with balance chord on NACA 0009 airfoil. Flap, 0.20c; gap, sealed and 0.005c. Tab, $0.20c_f$; gap, 0.001c; $\delta_t = 0°$.

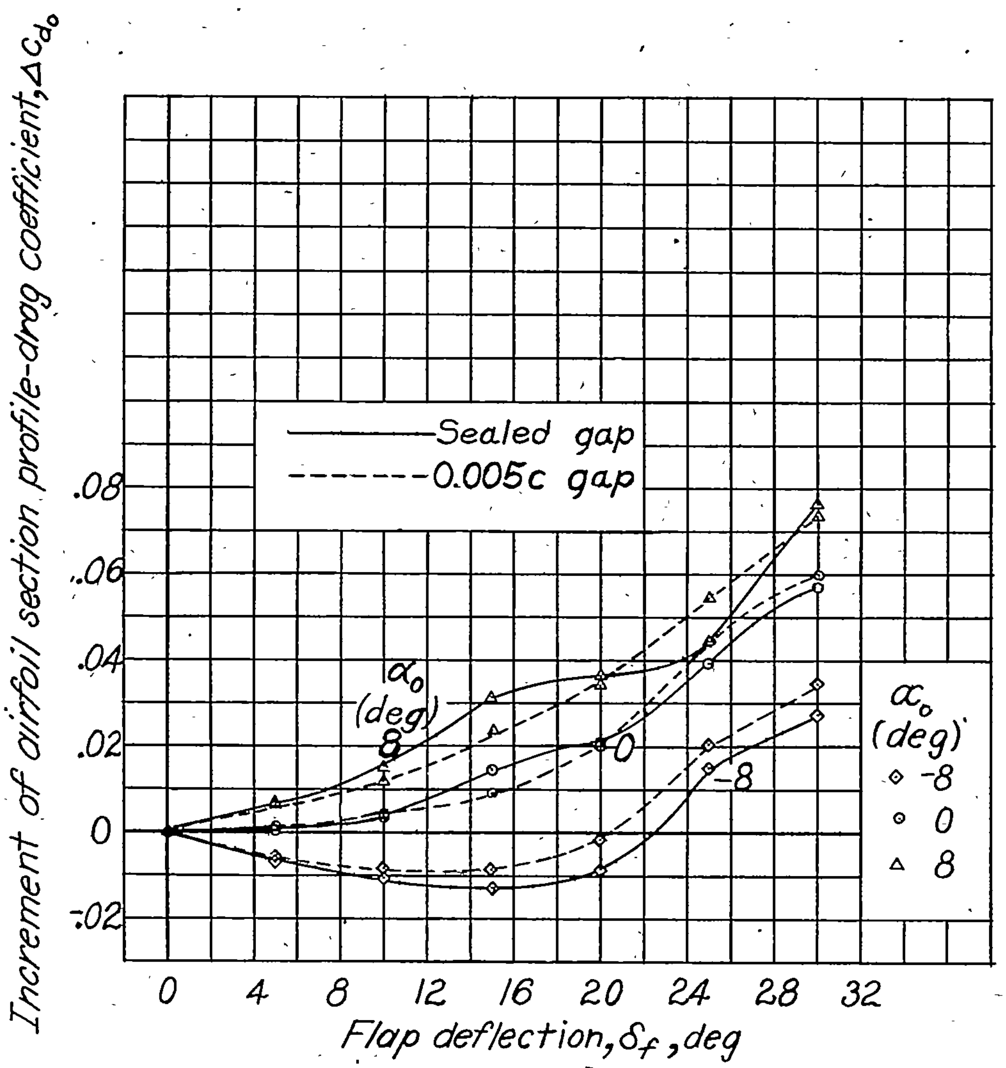

Figure 14.- Increment of airfoil section profile-drag coefficient caused by deflection of a 0.20c plain flap with gap sealed and with 0.005c gap. Tab, $0.20 c_f$; gap, 0.001c; $\delta_t = 0°$.

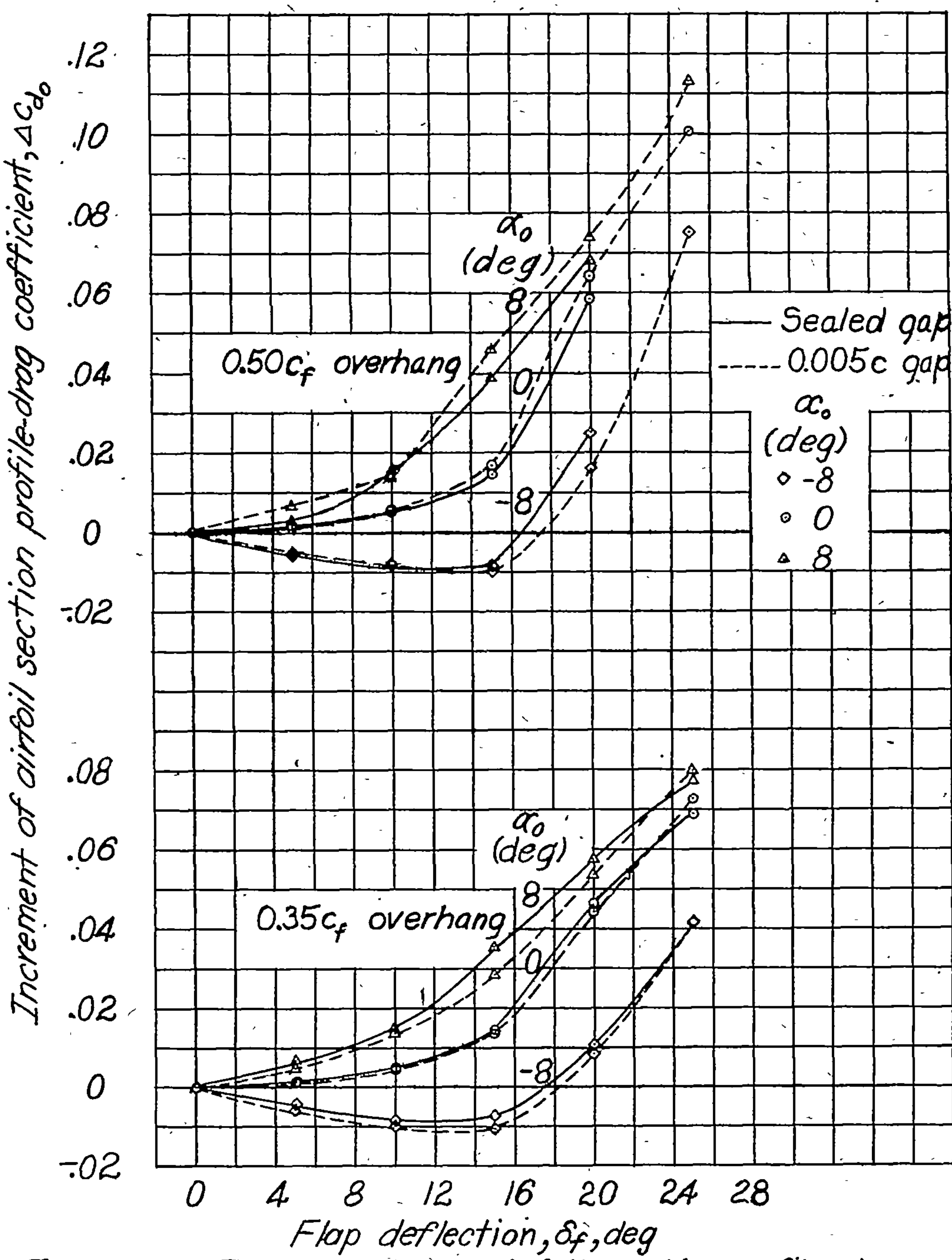

Figure 15.-Increment of airfoil section profile-drag coefficient caused by deflection of 0.20c flap having 0.35c_f and 0.50c_f blunt-nose overhangs with gap sealed and with 0.005c gap. Tab, 0.20 c_f; gap, 0.001c; $\delta_t = 0°$.

NATIONAL ADVISORY COMMITTEE FOR AERONAUTICS

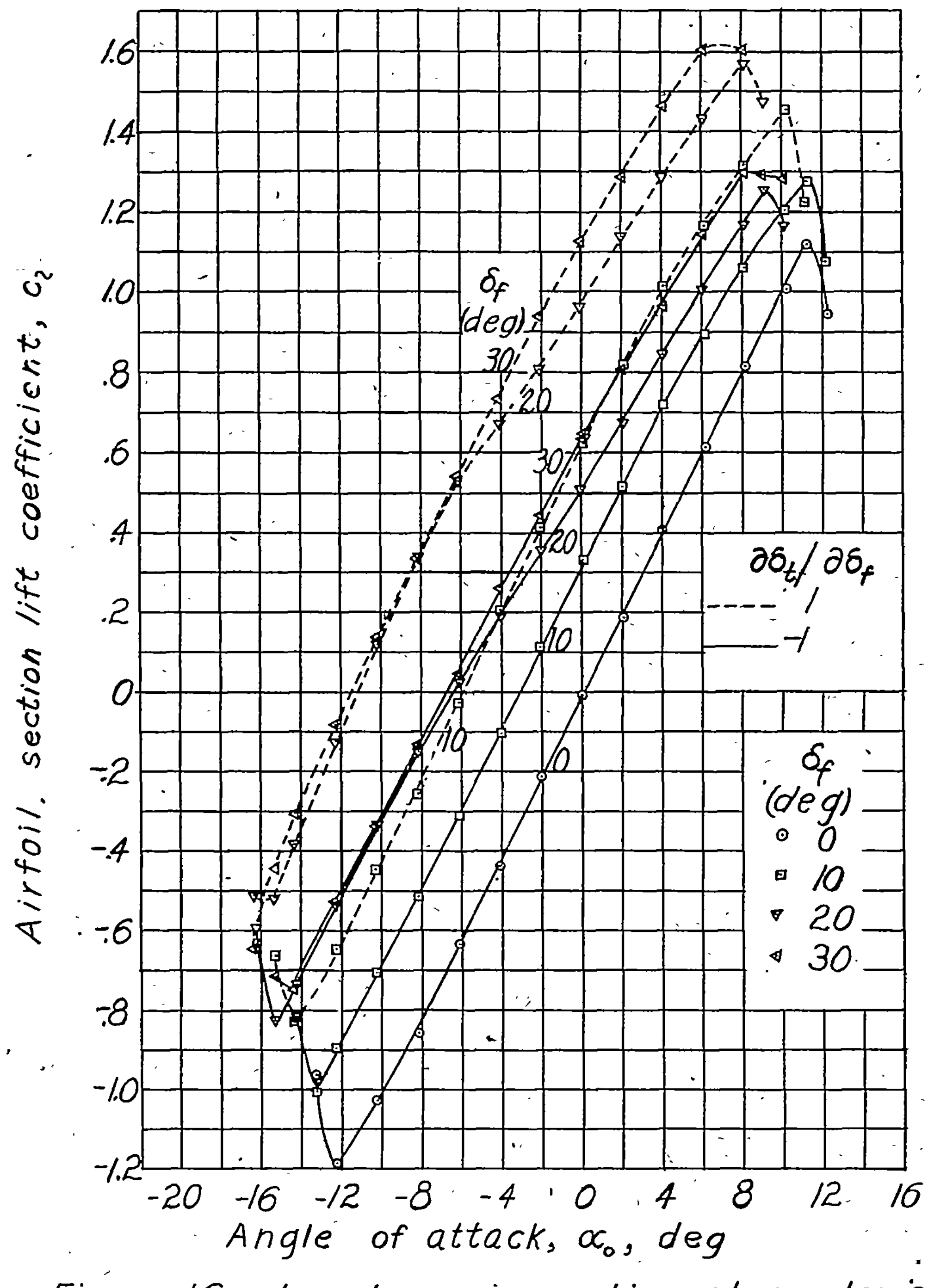

Figure 16.- Aerodynamic section characteristics of an NACA 0009 airfoil with a 0.20c plain flap having a $0.20c_f$ plain tab with $\frac{\partial\delta_t}{\partial\delta_f} = \pm 1$. Flap gap sealed; tab gap, 0.001c.

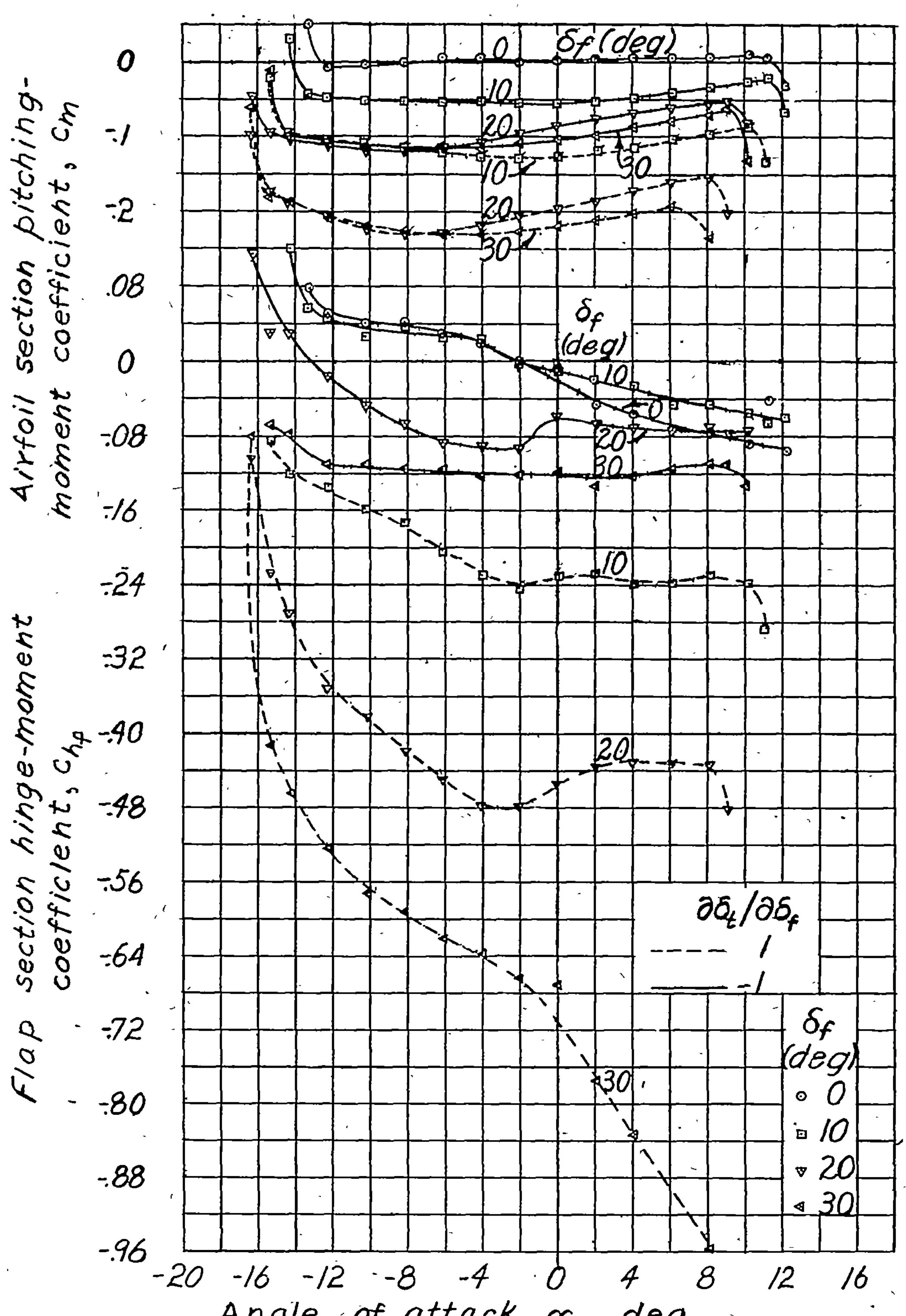

Figure 16 .- Continued.

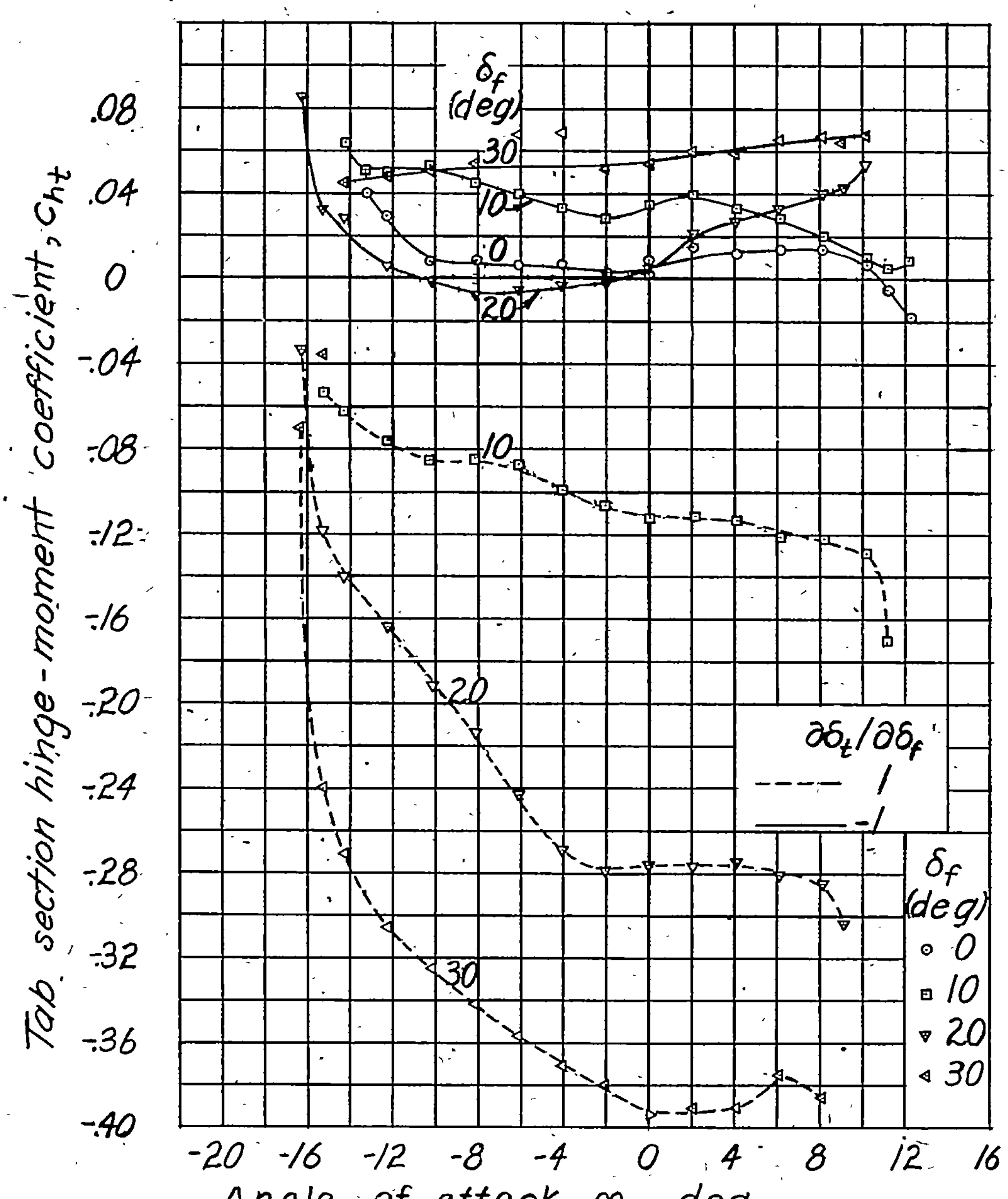

Figure 16.- Concluded.

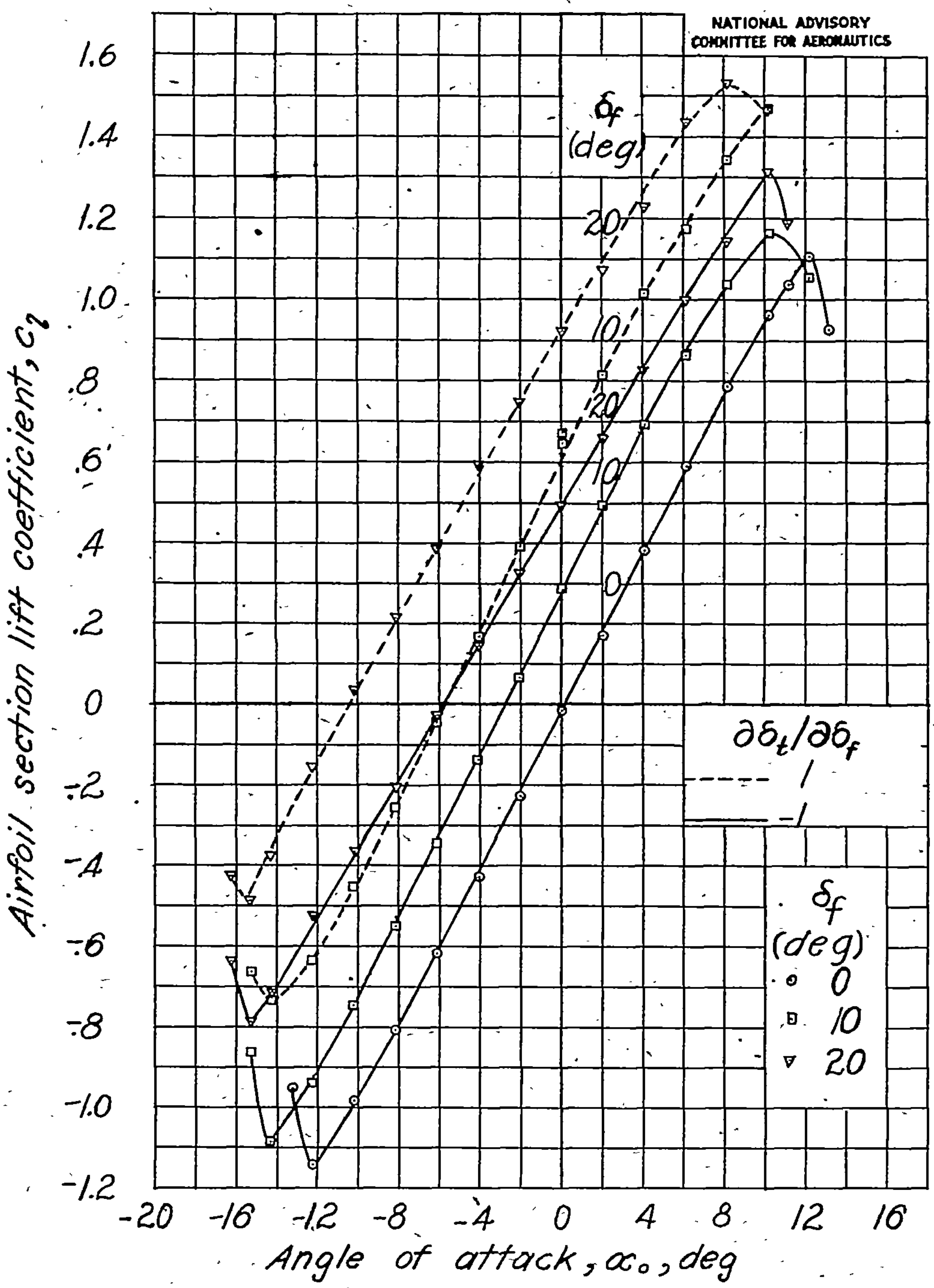

Figure 17.- Aerodynamic section characteristics of an NACA 0009 airfoil with a 0.20c flap having a $0.35c_f$ overhang with elliptical nose and $0.20c_f$ plain tab with $\frac{\partial\delta_t}{\partial\delta_f} = \pm 1$. Flap gap sealed; tab gap, 0.001c.

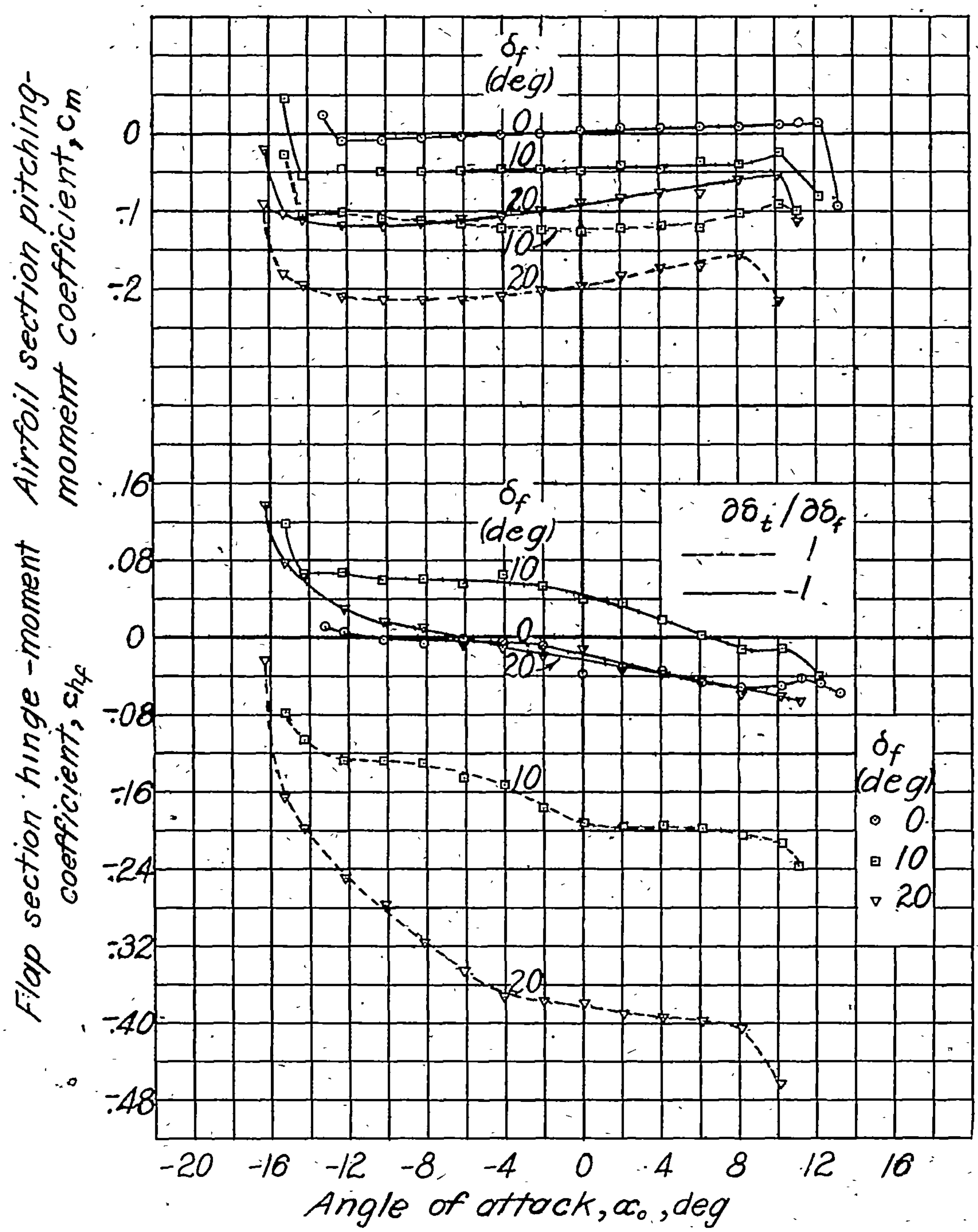

Figure 17.- Continued.

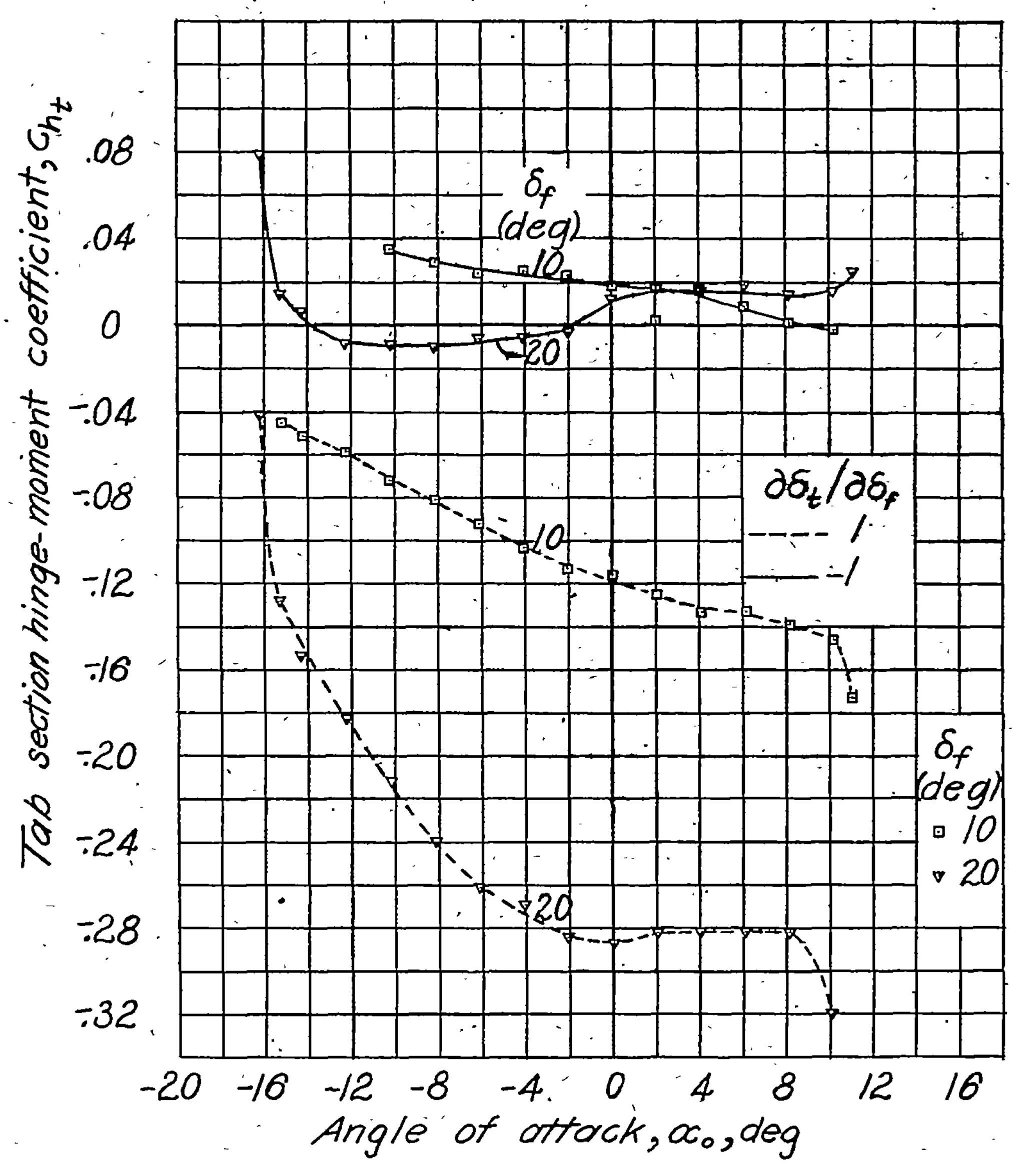

Figure 17 .- Concluded.

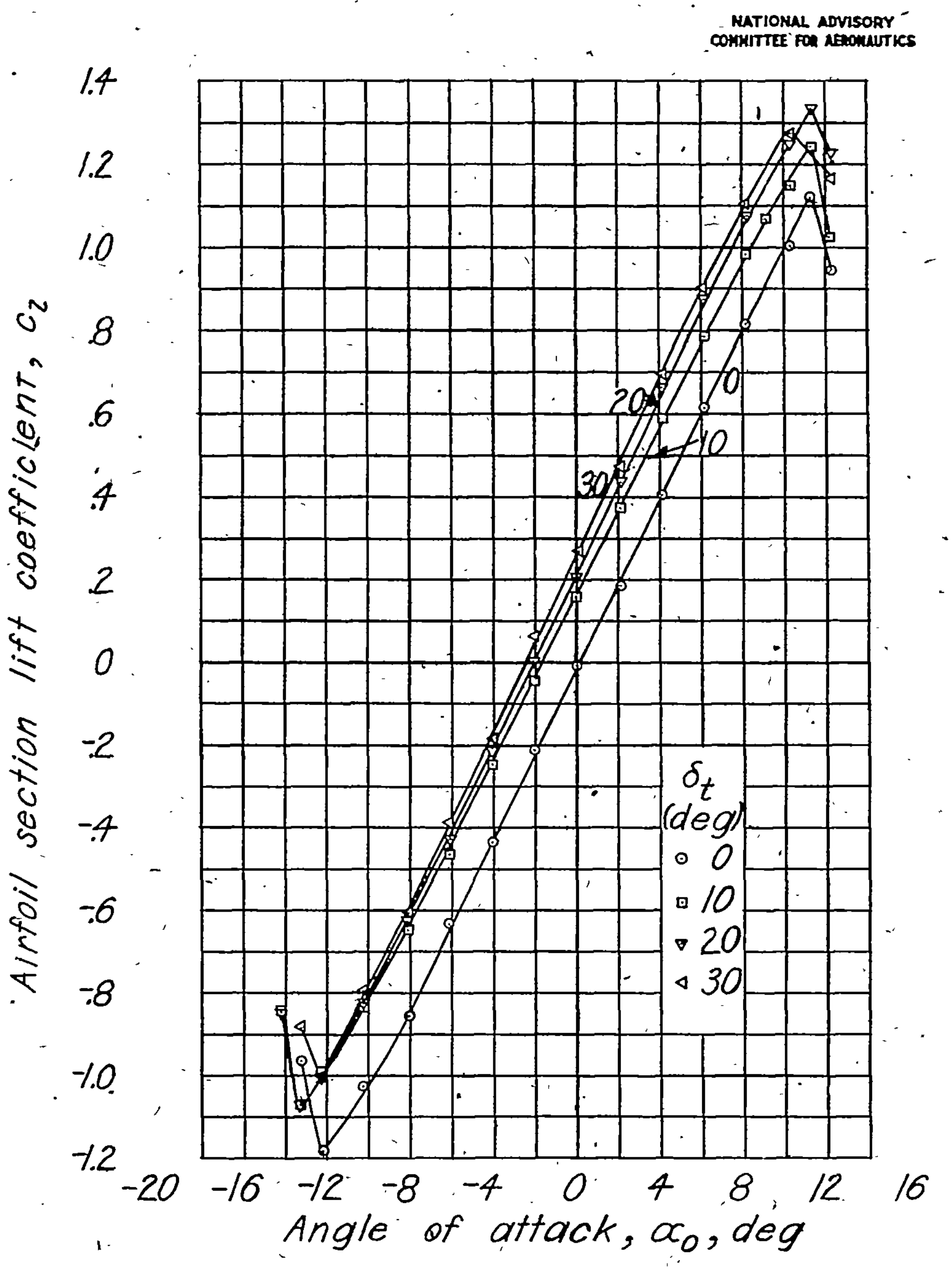

Figure 18.- Aerodynamic section characteristics of NACA 0009 airfoil with 0.20c plain flap having 0.20c_f plain tab. Flap gap, sealed; tab gap, 0.001c; $\delta_f = 0°$.

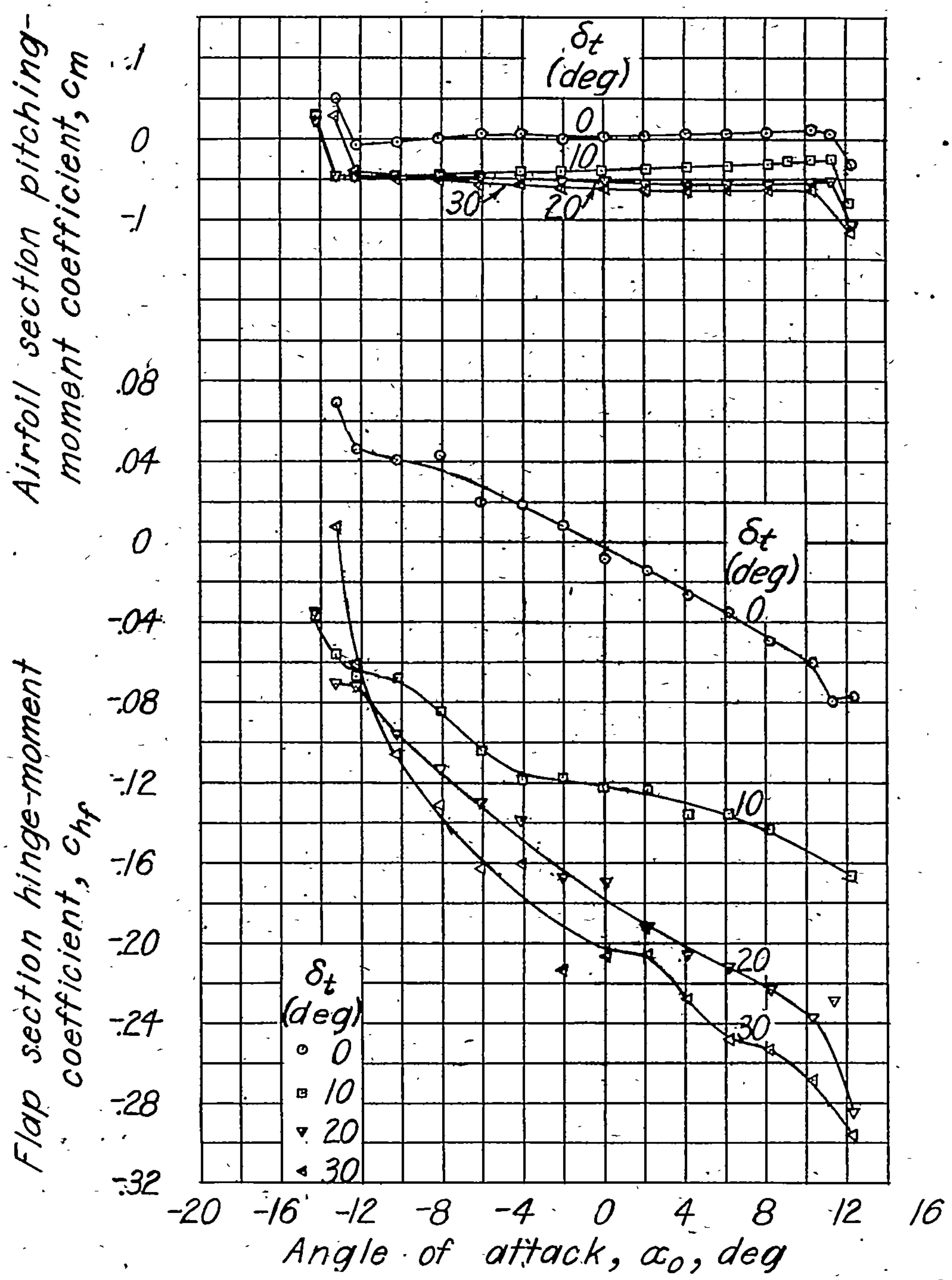

Figure 18.- Continued.

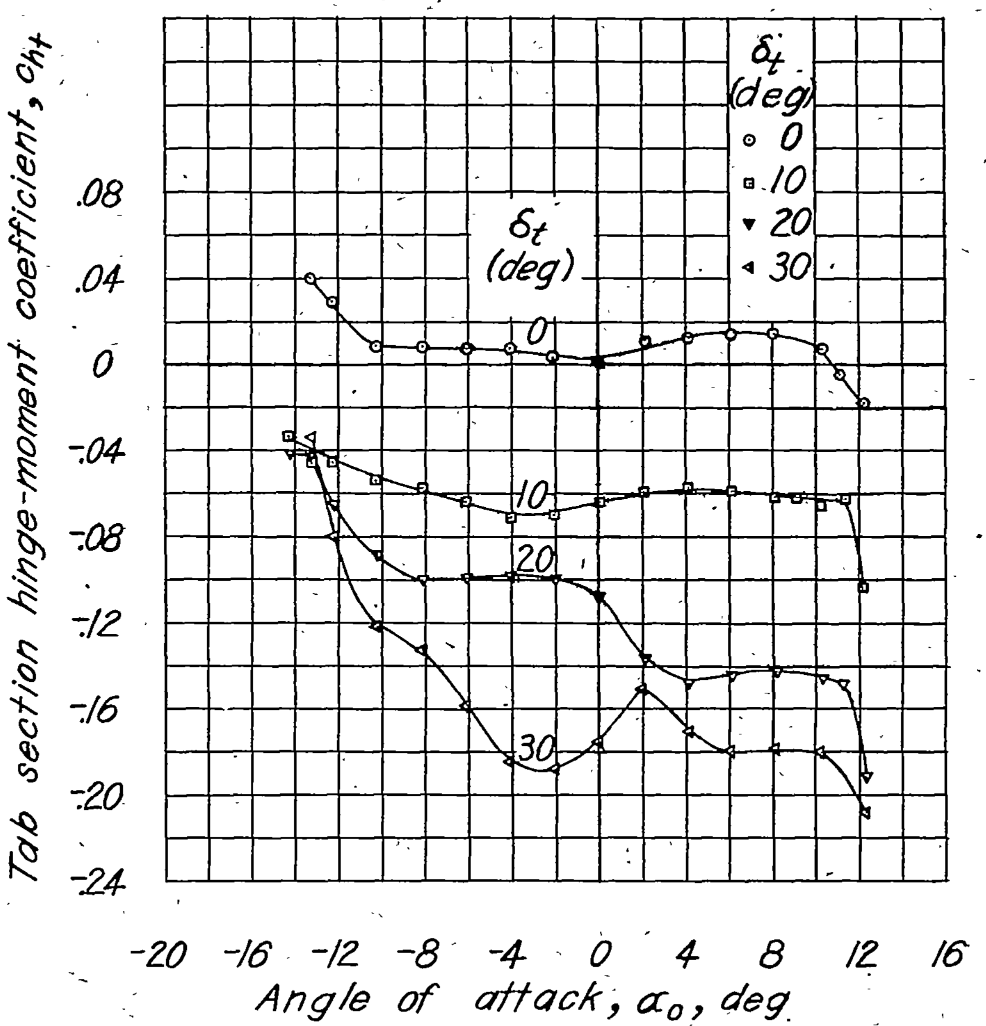

Figure 18.-Concluded.

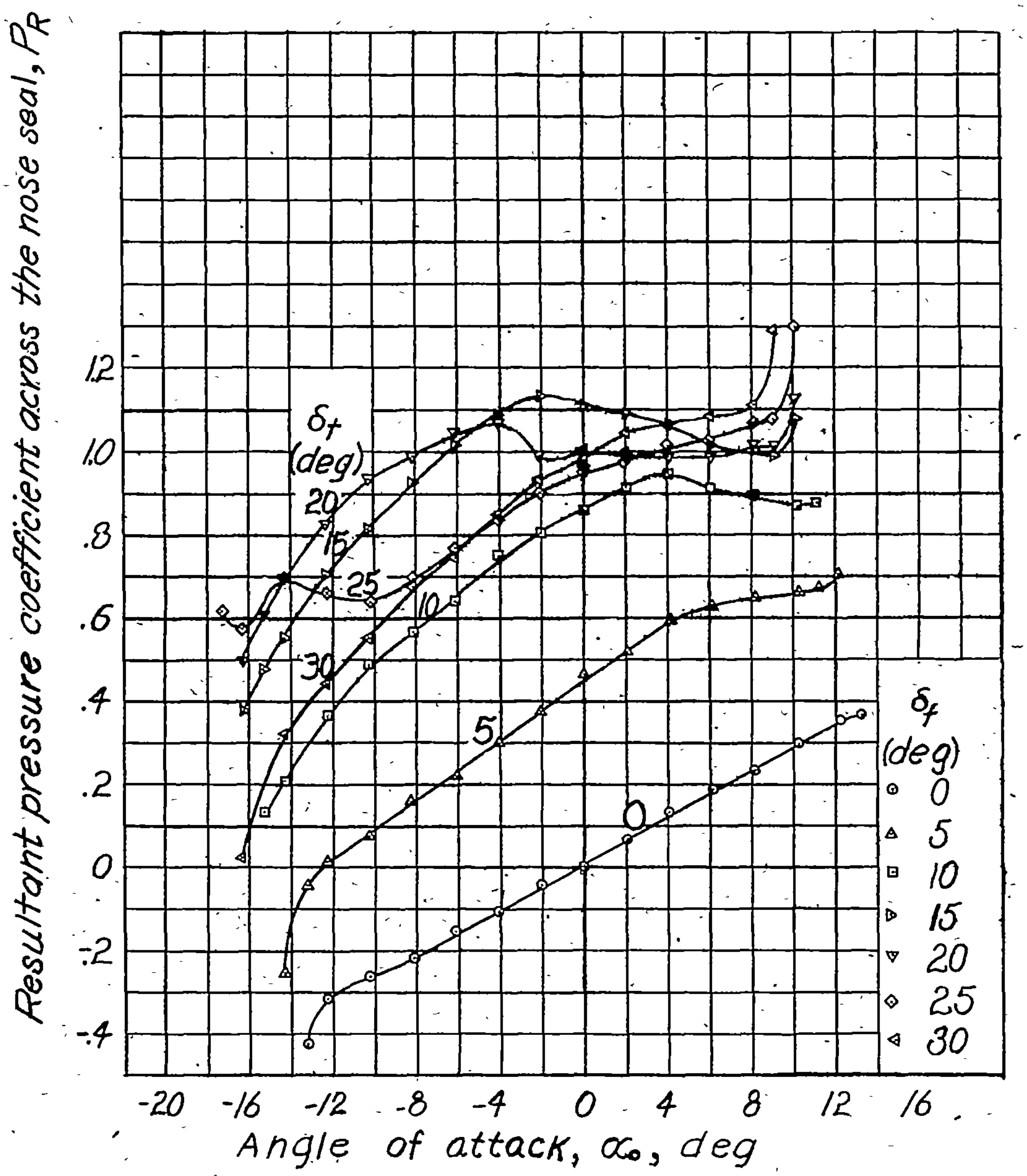

Figure 19.- Variation of resultant pressure coefficient across the 0.20c plain-flap nose seal with angle of attack on an NACA 0009 airfoil. Tab, $0.20c_f$; gap, 0.001c; $\delta_t = 0°$.

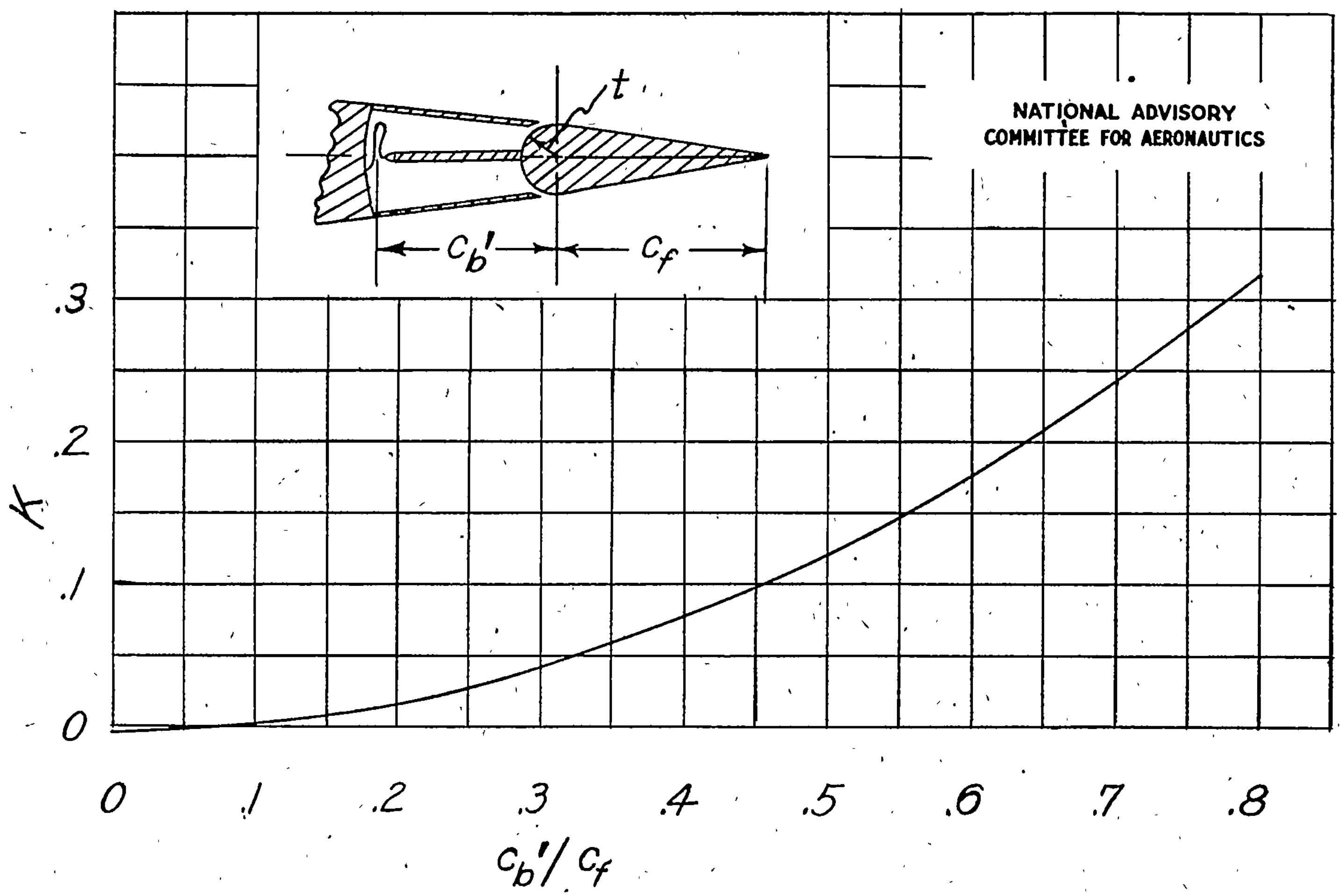

Figure 20.- Variation with internal-balance chord of constant K used in determining section hinge-moment coefficients of plain 0.20c flap fitted with internal balance. $K = \dfrac{\left(\dfrac{c_b'}{c_f}\right)^2 - \left(\dfrac{t}{c_f}\right)^2}{2}$.